

Computational Science Laboratory Report CSL-TR-19-5

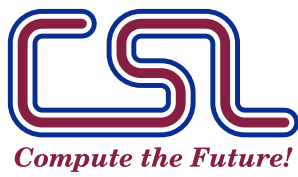
December 21, 2024

Steven Roberts, John Loffeld, Arash
Sarshar, Carol S. Woodward, and Adrian
Sandu

“Implicit multirate GARK methods”

Computational Science Laboratory
“Compute the Future!”

Department of Computer Science
Virginia Polytechnic Institute and State University
Blacksburg, VA 24060
Phone: (540)-231-2193
Fax: (540)-231-6075
Email: {steven94, sarshar}@vt.edu, {loffeld1,
woodward6}@llnl.gov, sandu@cs.vt.edu
Web: <http://csl.cs.vt.edu>



Implicit multirate GARK methods

Steven Roberts · John Loffeld · Arash
Sarshar · Carol S. Woodward · Adrian
Sandu

Received: December 21, 2024/ Accepted: date

Abstract This work considers multirate generalized-structure additively partitioned Runge–Kutta (MrGARK) methods for solving stiff systems of ordinary differential equations (ODEs) with multiple time scales. These methods treat different partitions of the system with different timesteps for a more targeted and efficient solution compared to monolithic single rate approaches. With implicit methods used across all partitions, methods must find a balance between stability and the cost of solving nonlinear equations for the stages. In order to characterize this important trade-off, we explore multirate coupling strategies, problems for assessing linear stability, and techniques to efficiently implement Newton iterations for stage equations. Unlike much of the existing multirate stability analysis which is limited in scope to particular methods, we present general statements on stability and describe fundamental limitations for certain types of multirate schemes. New implicit multirate methods up to fourth order are derived, and their accuracy and efficiency properties are verified with numerical tests.

Keywords Multirate · Time integration · Implicit methods

Mathematics Subject Classification (2010) 65L06 · 65L20

1 Introduction

In many real-world dynamical systems, there are parts of the system that evolve at significantly faster rates than other parts of the system. Traditional time integration methods, which take a uniform timestep across all parts of the system, can

S. Roberts · A. Sarshar
VirginiaTech
E-mail: {steven94, sarshar}@vt.edu

J. Loffeld · C.S. Woodward
Lawrence Livermore National Laboratory
E-mail: {loffeld1, woodward6}@llnl.gov

A. Sandu
VirginiaTech
E-mail: sandu@cs.vt.edu

struggle for this type of problem as the timestep must accommodate the fastest dynamics. Instead of treating such a system as a black box, many methods consider the fast and slow processes independently:

$$y' = f(y) = f^{\{f\}}(y) + f^{\{s\}}(y), \quad y(t_0) = y_0, \quad y(t) \in \mathbb{R}^d. \quad (1)$$

An important special case of this additively partitioned system is the component partitioned problem

$$\begin{bmatrix} y^{\{f\}} \\ y^{\{s\}} \end{bmatrix}' = \begin{bmatrix} f^{\{f\}}(y^{\{f\}}, y^{\{s\}}) \\ f^{\{s\}}(y^{\{f\}}, y^{\{s\}}) \end{bmatrix}, \quad (2)$$

with $y^{\{f\}} \in \mathbb{R}^{d^{\{f\}}}$, $y^{\{s\}} \in \mathbb{R}^{d^{\{s\}}}$, and $d = d^{\{f\}} + d^{\{s\}}$.

Multirate methods efficiently solve the system of ordinary differential equations (ODEs) eq. (1) by integrating the fast dynamics $f^{\{f\}}$ with a smaller timestep than the slow dynamics $f^{\{s\}}$. The choice of how to partition f into $f^{\{f\}}$ and $f^{\{s\}}$ can depend on many factors including stiffness, accuracy requirements, cost of evaluation, linearity, and memory requirements. In the case where an implicit method is needed, which will be the focus of this paper, the cost and convergence of the nonlinear solver also comes into consideration. There may be a small number of components of an ODE that cause slow convergence of a single rate Newton iteration (e.g. a boundary layer). Such components can be grouped into $f^{\{f\}}$. In some cases, the Jacobian of f is an unstructured matrix leading to expensive linear solves, but the problem can be decomposed such that linear solves with the Jacobians of $f^{\{f\}}$ and $f^{\{s\}}$ are inexpensive.

Implicit methods require excellent stability to offset the cost of solving potentially nonlinear equations in each step. For this reason, an understanding of the stability of multirate methods is crucial. One of the first works studying multirate stability was that of Gear [6]. Subsequent authors have examined multirate stability in the context of backward Euler [20, 28, 31], Runge–Kutta methods [2, 13, 12], linear multistep methods [7, 28, 32], and Rosenbrock methods [8, 19, 24].

Much of the development of multirate schemes for stiff systems has focused on multirate Rosenbrock methods, but methods based on implicit Runge–Kutta methods have been explored as well. In [12], a multirate θ -method is presented and analyzed. Recently, multirate methods based on TR-BDF2 were proposed in [5, 3]. In [21, 18], new strategies for creating implicit multirate infinitesimal methods were introduced.

In [22], Sandu and Günther propose the generalized-structure additively partitioned Runge–Kutta (GARK) family of methods. GARK provides a unifying framework that includes traditional, implicit-explicit (IMEX), and multirate Runge–Kutta methods. Order conditions as well as the linear and nonlinear stability analysis are developed for this large class of methods. Günther and Sandu continue in [9] where many variants of multirate Runge–Kutta methods are cast as GARK methods. Multirate GARK (MrGARK) methods up to order four are derived in [23]. These include methods that are explicit in both partitions and methods that combine explicit and implicit methods.

In this work, we develop new MrGARK methods that are implicit in both the fast and slow partitions. The development is guided by new theoretical results regarding the stability of multirate methods. Necessary and sufficient conditions

for achieving A-stability are presented, as well as some fundamental stability limitations on certain types of multirate methods. Many of these results extend past multirate methods to the entire GARK framework. Numerical experiments verify the order of convergence and the efficiency of the new schemes.

The structure of this paper is as follows. Section 2 introduces multirate methods using the GARK framework. The linear stability of multirate methods is explored in section 3. Section 4 discusses techniques to efficiently implement the Newton iterations. Section 5 contains the newly derived implicit MrGARK methods, and section 6 presents the numerical experiments used to test the methods. Finally, we summarize the results of the paper in section 7.

2 Multirate GARK methods

The GARK framework [22] is used as the foundation for representing and analyzing multirate Runge–Kutta methods. In the most general form for a two-partitioned system eq. (1), one step reads

$$Y_i^{\{f\}} = y_n + H \sum_{j=1}^{s^{\{f\}}} a_{i,j}^{\{f,f\}} f^{\{f\}}(Y_j^{\{f\}}) + H \sum_{j=1}^{s^{\{s\}}} a_{i,j}^{\{f,s\}} f^{\{s\}}(Y_j^{\{s\}}), \quad (3a)$$

for $i = 1, \dots, s^{\{f\}}$,

$$Y_i^{\{s\}} = y_n + H \sum_{j=1}^{s^{\{s\}}} a_{i,j}^{\{s,s\}} f^{\{s\}}(Y_j^{\{s\}}) + H \sum_{j=1}^{s^{\{f\}}} a_{i,j}^{\{s,f\}} f^{\{f\}}(Y_j^{\{f\}}), \quad (3b)$$

for $i = 1, \dots, s^{\{s\}}$,

$$y_{n+1} = y_n + H \sum_{j=1}^{s^{\{f\}}} b_j^{\{f\}} f^{\{f\}}(Y_j^{\{f\}}) + H \sum_{j=1}^{s^{\{s\}}} b_j^{\{s\}} f^{\{s\}}(Y_j^{\{s\}}). \quad (3c)$$

The coefficients of these methods can be organized into the following Butcher tableau:

$$\begin{array}{c|c} \mathbf{A}^{\{f,f\}} & \mathbf{A}^{\{f,s\}} \\ \hline \mathbf{A}^{\{s,f\}} & \mathbf{A}^{\{s,s\}} \\ \hline \mathbf{b}^{\{f\}T} & \mathbf{b}^{\{s\}T} \end{array} \quad (4)$$

The fast method $(\mathbf{A}^{\{f,f\}}, \mathbf{b}^{\{f\}}, \mathbf{c}^{\{f\}})$ has $s^{\{f\}}$ stages, and the slow method $(\mathbf{A}^{\{s,s\}}, \mathbf{b}^{\{s\}}, \mathbf{c}^{\{s\}})$, has $s^{\{s\}}$ stages. Also, we use the notation

$$\mathbf{A} = \begin{bmatrix} \mathbf{A}^{\{f,f\}} & \mathbf{A}^{\{f,s\}} \\ \mathbf{A}^{\{s,f\}} & \mathbf{A}^{\{s,s\}} \end{bmatrix}, \quad \mathbf{b} = \begin{bmatrix} \mathbf{b}^{\{f\}} \\ \mathbf{b}^{\{s\}} \end{bmatrix}, \quad \mathbf{s} = \mathbf{s}^{\{f\}} + \mathbf{s}^{\{s\}}.$$

A common simplifying assumption, which ensures the fast and slow functions in eq. (3) are computed at consistent times, is internal consistency:

$$\mathbf{c}^{\{f\}} := \mathbf{A}^{\{f,f\}} \mathbf{1}_{s^{\{f\}}} = \mathbf{A}^{\{f,s\}} \mathbf{1}_{s^{\{s\}}} \quad \text{and} \quad \mathbf{c}^{\{s\}} := \mathbf{A}^{\{s,s\}} \mathbf{1}_{s^{\{s\}}} = \mathbf{A}^{\{s,f\}} \mathbf{1}_{s^{\{f\}}}. \quad (5)$$

In [9], it was shown how several types of multirate Runge–Kutta methods can be described as GARK methods. In one step of a multirate method, the slow dynamics $f^{\{s\}}$ are integrated with a stepsize of H , and the fast dynamics $f^{\{f\}}$ are integrated with a stepsize $h = H/M$. The multirate ratio M is a positive integer. Information between the two partitions is shared via the coupling matrices $\mathbf{A}^{\{f,s\}}$ and $\mathbf{A}^{\{s,f\}}$. In this section, we present two primary types of multirate Runge–Kutta methods.

2.1 Standard MrGARK

A standard MrGARK method is built on an $s^{\{f\}}$ -stage fast base method $(A^{\{f,f\}}, b^{\{f\}}, c^{\{f\}})$ and an $s^{\{s\}}$ -stage slow base method $(A^{\{s,s\}}, b^{\{s\}}, c^{\{s\}})$. From [9], one step proceeds as follows:

$$Y_i^{\{s\}} = y_n + H \sum_{j=1}^{s^{\{s\}}} a_{i,j}^{\{s,s\}} f^{\{s\}}(Y_j^{\{s\}}) + h \sum_{\lambda=1}^M \sum_{j=1}^{s^{\{f\}}} a_{i,j}^{\{s,f,\lambda\}} f^{\{f\}}(Y_j^{\{f,\lambda\}}), \quad (6a)$$

for $i = 1, \dots, s^{\{s\}}$,

$$Y_i^{\{f,\lambda\}} = \tilde{y}_{n+(\lambda-1)/M} + H \sum_{j=1}^{s^{\{s\}}} a_{i,j}^{\{f,s,\lambda\}} f^{\{s\}}(Y_j^{\{s\}}) + h \sum_{j=1}^{s^{\{f\}}} a_{i,j}^{\{f,f\}} f^{\{f\}}(Y_j^{\{f,\lambda\}}),$$

for $i = 1, \dots, s^{\{f\}}$,

$$\tilde{y}_{n+\lambda/M} = \tilde{y}_{n+(\lambda-1)/M} + h \sum_{i=1}^{s^{\{f\}}} b_i^{\{f\}} f^{\{f\}}(Y_i^{\{f,\lambda\}}),$$

for $\lambda = 1, \dots, M$,

(6b)

$$y_{n+1} = \tilde{y}_{n+M/M} + H \sum_{i=1}^{s^{\{s\}}} b_i^{\{s\}} f^{\{s\}}(Y_i^{\{s\}}), \quad (6c)$$

where the micro-steps start with $\tilde{y}_n = y_n$. The corresponding Butcher tableau for eq. (6) is

$$\begin{array}{c|ccccc} & \frac{1}{M} A^{\{f,f\}} & \dots & 0 & A^{\{f,s,1\}} \\ \hline \mathbf{A}^{\{f,f\}} & \mathbf{A}^{\{f,s\}} & & & \vdots \\ \hline \mathbf{A}^{\{s,f\}} & \mathbf{A}^{\{s,s\}} & & & A^{\{f,s,M\}} \\ \hline \mathbf{b}^{\{f\}T} & \mathbf{b}^{\{s\}T} & & & A^{\{s,s\}} \\ & \frac{1}{M} A^{\{s,f,1\}} & \dots & A^{\{s,f,M\}} & \\ & \frac{1}{M} b^{\{f\}T} & \dots & \frac{1}{M} b^{\{f\}T} & b^{\{s\}T} \end{array} \quad (7)$$

Note that $s^{\{f\}} = Ms^{\{f\}}$ and $s^{\{s\}} = s^{\{s\}}$.

If the fast and slow base methods are identical, the method is called *telescopic* as it can be applied in a nested fashion to more than two partitions [9]. Further, MrGARK methods can be classified as coupled or decoupled [23]. Decoupled methods only have implicitness in the base methods; the stages used in coupling can

always be computed before they are needed. Coupled methods, on the other hand, have fast and slow stages which depend on each other. Decoupled methods can be implemented more efficiently, but can sacrifice stability as we will see in section 3.

Order conditions for this family of methods comes from applying the particular multirate structure of eq. (7) into the GARK order conditions. The conditions up to order four are provided in [23]. A similar tableau structure is used to describe and derive order conditions for multirate infinitesimal step methods [22, 27] and the more general MRI-GARK framework [21].

2.2 Compound-step MrGARK methods

Another multirate strategy, based on the early work of Rice [17] and the later developments in [25, 31], is the compound-step approach. The idea is to first take a macro-step of the full system eq. (1) called the compound step. Over the large timestep, the fast integration is inaccurate and discarded. The fast partition is then reintegrated using a smaller timestep. Slow coupling information is required at the intermediate micro-steps and can come from an interpolant of the compound step solution. Note the fast partition is integrated twice for each timestep, but no extrapolation is required for the coupling. Moreover, an error estimate from the compound step, say from an embedded method, can be used to dynamically determine at each step which variables exceed accuracy tolerances and should form the fast components [25].

Traditionally, compound-step methods have been posed for component partitioned systems eq. (2), however, they easily extend to additively partitioned systems eq. (1). One step of a compound-step MrGARK scheme is given by

$$Y_i = y_n + H \sum_{j=1}^s a_{i,j} f(Y_i), \quad i = 1, \dots, s, \quad (8a)$$

$$Y_i^{\{f,\lambda\}} = \tilde{y}_{n+(\lambda-1)/M} + h \sum_{j=1}^{s^{\{f\}}} a_{i,j}^{\{f,f\}} f^{\{f\}}(Y_j^{\{f,\lambda\}}) + H \sum_{j=1}^{s^{\{s\}}} a_{i,j}^{\{f,s,\lambda\}} f^{\{s\}}(Y_j),$$

for $i = 1, \dots, s^{\{f\}}$, (8b)

$$\tilde{y}_{n+\lambda/M} = \tilde{y}_{n+(\lambda-1)/M} + h \sum_{i=1}^{s^{\{f\}}} b_i^{\{f\}} f^{\{f\}}(Y_i^{\{f,\lambda\}}),$$

for $\lambda = 1, \dots, M$, (8c)

$$y_{n+1} = \tilde{y}_{n+M/M} + H \sum_{i=1}^{s^{\{s\}}} b_i^{\{s\}} f^{\{s\}}(Y_i),$$

where the micro-steps start with $\tilde{y}_n = y_n$. The corresponding tableau is

$$\begin{array}{c|c} \begin{array}{c|c} A & 0 \\ \hline \mathbf{A}^{\{\mathfrak{f},\mathfrak{f}\}} & \mathbf{A}^{\{\mathfrak{f},\mathfrak{s}\}} \end{array} & \begin{array}{c|c} A & \\ \hline 0 & \frac{1}{M}A \end{array} \\ \hline \begin{array}{c|c} \mathbf{A}^{\{\mathfrak{s},\mathfrak{f}\}} & \mathbf{A}^{\{\mathfrak{s},\mathfrak{s}\}} \\ \hline \mathbf{b}^{\{\mathfrak{f}\}T} & \mathbf{b}^{\{\mathfrak{s}\}T} \end{array} & \begin{array}{c|c} \vdots & \ddots \\ \hline 0 & \frac{1}{M}\mathbb{1}_s b^T \end{array} \end{array} \begin{array}{c|c} & A^{\{\mathfrak{f},\mathfrak{s},1\}} \\ \hline & \vdots \\ \hline & A^{\{\mathfrak{f},\mathfrak{s},M\}} \\ \hline \begin{array}{c|c} A & 0 \\ \hline 0 & \frac{1}{M}b^T \end{array} & \begin{array}{c|c} A & \\ \hline b^T & \end{array} \end{array}$$

This family of methods is telescopic, coupled in the macro-step eq. (8a), and decoupled in the remaining fast micro-steps eq. (8b). The coupling matrix $A^{\{\mathfrak{f},\mathfrak{s},\lambda\}}$ can be interpreted as the interpolation weights for the slow tendencies. These multirate methods will preserve the order of the base method if the interpolant is sufficiently accurate. We note that this is a sufficient condition, but not always necessary. The GARK order conditions can be used to derive precise conditions to achieve a particular order.

Theorem 1 (Compound-step MrGARK order conditions). *An internally consistent compound-step MrGARK method has order four if and only if the base method (A, b) has order four and the following coupling conditions hold:*

$$M A^{\{\mathfrak{f},\mathfrak{s},\lambda\}} \mathbb{1}_{s^{\{\mathfrak{s}\}}} = (\lambda - 1) \mathbb{1}_{s^{\{\mathfrak{f}\}}} + c, \quad (i.c) \quad (9a)$$

$$\frac{M}{6} = \sum_{\lambda=1}^M b^T A^{\{\mathfrak{f},\mathfrak{s},\lambda\}} c, \quad (\text{order 3}) \quad (9b)$$

$$\frac{M^2}{8} = \sum_{\lambda=1}^M (\lambda - 1) b^T A^{\{\mathfrak{f},\mathfrak{s},\lambda\}} c + \sum_{\lambda=1}^M (b \times c)^T A^{\{\mathfrak{f},\mathfrak{s},\lambda\}} c, \quad (\text{order 4}) \quad (9c)$$

$$\frac{M}{12} = \sum_{\lambda=1}^M b^T A^{\{\mathfrak{f},\mathfrak{s},\lambda\}} c^2, \quad (\text{order 4}) \quad (9d)$$

$$\frac{M^2}{24} = \sum_{\lambda=1}^M b^T A A^{\{\mathfrak{f},\mathfrak{s},\lambda\}} c + \sum_{\lambda=1}^M (M - \lambda) b^T A^{\{\mathfrak{f},\mathfrak{s},\lambda\}} c, \quad (\text{order 4}) \quad (9e)$$

$$\frac{M}{24} = \sum_{\lambda=1}^M b^T A^{\{\mathfrak{f},\mathfrak{s},\lambda\}} A c. \quad (\text{order 4}) \quad (9f)$$

Proof. From [22], an internally consistent GARK method has order four if and only the base methods have order four and the following coupling conditions hold.

Condition 3a:

$$\frac{1}{6} = \mathbf{b}^{\{\mathfrak{f}\}T} \mathbf{A}^{\{\mathfrak{f},\mathfrak{s}\}} \mathbf{c}^{\{\mathfrak{s}\}} = \frac{1}{M} \sum_{\lambda=1}^M b^T A^{\{\mathfrak{f},\mathfrak{s},\lambda\}} c.$$

Condition 3b:

$$\frac{1}{6} = \mathbf{b}^{\{\mathfrak{s}\}T} \mathbf{A}^{\{\mathfrak{s},\mathfrak{f}\}} \mathbf{c}^{\{\mathfrak{f}\}} = b^T A c.$$

Condition 4a:

$$\begin{aligned} \frac{1}{8} &= \left(\mathbf{b}^{\{f\}} \times \mathbf{c}^{\{f\}} \right)^T \mathbf{A}^{\{f,s\}} \mathbf{c}^{\{s\}} \\ &= \frac{1}{M^2} \sum_{\lambda=1}^M (b \times (c + (\lambda - 1) \mathbf{1}_s))^T A^{\{f,s,\lambda\}} c^{\{s\}}. \\ &= \frac{1}{M^2} \sum_{\lambda=1}^M (\lambda - 1) b^T A^{\{f,s,\lambda\}} c + \frac{1}{M^2} \sum_{\lambda=1}^M (b \times c)^T A^{\{f,s,\lambda\}} c \end{aligned}$$

Condition 4b:

$$\frac{1}{8} = \left(\mathbf{b}^{\{s\}} \times \mathbf{c}^{\{s\}} \right)^T \mathbf{A}^{\{s,f\}} \mathbf{c}^{\{f\}} = (b \times c)^T A c.$$

Condition 4c:

$$\frac{1}{12} = \mathbf{b}^{\{f\}T} \mathbf{A}^{\{f,s\}} \mathbf{c}^{\{s\} \times 2} = \frac{1}{M} \sum_{\lambda=1}^M b^T A^{\{f,s,\lambda\}} c^2.$$

Condition 4d:

$$\frac{1}{12} = \mathbf{b}^{\{s\}T} \mathbf{A}^{\{s,f\}} \mathbf{c}^{\{f\} \times 2} = b^T A c^2.$$

Condition 4e:

$$\begin{aligned} \frac{1}{24} &= \mathbf{b}^{\{f\}T} \mathbf{A}^{\{f,f\}} \mathbf{A}^{\{f,s\}} \mathbf{c}^{\{s\}} \\ &= \frac{1}{M^2} \sum_{\lambda=1}^M \left(b^T A + \sum_{k=1}^{M-\lambda} b^T \mathbf{1}_s b^T \right) A^{\{f,s,\lambda\}} c \\ &= \frac{1}{M^2} \sum_{\lambda=1}^M b^T A A^{\{f,s,\lambda\}} c + \frac{1}{M^2} \sum_{\lambda=1}^M (M - \lambda) b^T A^{\{f,s,\lambda\}} c. \end{aligned}$$

Condition 4f:

$$\frac{1}{24} = \mathbf{b}^{\{f\}T} \mathbf{A}^{\{f,s\}} \mathbf{A}^{\{s,f\}} \mathbf{c}^{\{f\}} = \frac{1}{M} \sum_{\lambda=1}^M b^T A^{\{f,s,\lambda\}} A c.$$

Condition 4g:

$$\frac{1}{24} = \mathbf{b}^{\{f\}T} \mathbf{A}^{\{f,s\}} \mathbf{A}^{\{s,s\}} \mathbf{c}^{\{s\}} = \frac{1}{M} \sum_{\lambda=1}^M b^T A^{\{f,s,\lambda\}} A c.$$

Condition 4h:

$$\frac{1}{24} = \mathbf{b}^{\{s\}T} \mathbf{A}^{\{s,s\}} \mathbf{A}^{\{s,f\}} \mathbf{c}^{\{f\}} = b^T A A c.$$

Condition 4i:

$$\frac{1}{24} = \mathbf{b}^{\{s\}T} \mathbf{A}^{\{s,f\}} \mathbf{A}^{\{f,s\}} \mathbf{c}^{\{s\}} = b^T A A c.$$

Condition 4j:

$$\frac{1}{24} = \mathbf{b}^{\{s\}T} \mathbf{A}^{\{s,f\}} \mathbf{A}^{\{f,f\}} \mathbf{c}^{\{f\}} = b^T A A c.$$

Note that conditions 3b, 4b, 4d, and 4h–j resolve to order conditions of the base method, and thus, are satisfied if and only if the base method has order four. Further, condition 4g is identical to 4f. The remaining order conditions give eq. (9). \square

3 Multirate linear stability analysis

In the analysis of single rate Runge–Kutta methods, it is common to apply methods to the Dahlquist test problem

$$y' = \lambda y, \quad (10)$$

with $\lambda \in \mathbb{C}^- = \{z \in \mathbb{C} : \operatorname{Re}(z) \leq 0\}$. This yields the well-known stability function

$$R(z) = 1 + z b^T (I - z A)^{-1} \mathbf{1}_s, \quad (11)$$

where $z = \lambda h$. It suffices to only examine a scalar problem eq. (10) because in the case λ and z are matrices, the behavior of $R(z)^m$ as $m \rightarrow \infty$ only depends on the scalar eigenvalues of z . That is, the choice of basis for a system of linear ODEs does not affect a Runge–Kutta method’s stability.

As noted by Gear [7], this property does not hold for multirate and other partitioned schemes. For this reason, the stability analysis becomes significantly more complex. In this section, we analyze and compare linear stability for both scalar and two-dimensional (2D) test problems. The scalar test problem is a simple model of an additively partitioned system (1) where the Jacobians of the two processes triagularize simultaneously. The 2D problem is a simple model for a component partitioned system (2), where each component’s dynamics as well as the interaction between components are linear.

In this section, we will focus on two-partitioned GARK methods for simplicity. Nearly all of the stability analysis, however, has straightforward generalizations to the full N -partitioned GARK framework.

3.1 Scalar test problem

The simplest generalization of eq. (10) for two-partitioned multirate methods is the scalar test problem

$$y' = \lambda^{\{f\}} y + \lambda^{\{s\}} y, \quad (12)$$

where, $\lambda^{\{f\}}, \lambda^{\{s\}} \in \mathbb{C}^-$. As shown in [22], when eq. (6) is applied to eq. (12), we arrive at the stability function

$$R_1(z^{\{f\}}, z^{\{s\}}) = 1 + \mathbf{b}^T Z (I_{s \times s} - \mathbf{A} Z)^{-1} \mathbf{1}_s, \quad (13)$$

where $z^{\{f\}} = H \lambda^{\{f\}}$, $z^{\{s\}} = H \lambda^{\{s\}}$, and

$$Z = \begin{bmatrix} z^{\{f\}} I_{s^{\{f\}} \times s^{\{f\}}} & 0 \\ 0 & z^{\{s\}} I_{s^{\{s\}} \times s^{\{s\}}} \end{bmatrix}.$$

Definition 1 (Scalar region of absolute stability). *The set*

$$S_1 = \left\{ (z^{\{f\}}, z^{\{s\}}) \in \mathbb{C} \times \mathbb{C} : \left| R_1(z^{\{f\}}, z^{\{s\}}) \right| \leq 1 \right\}$$

is the region of absolute stability for the test problem eq. (12). A GARK method is called scalar A-stable if $S_1 \supseteq \mathbb{C}^- \times \mathbb{C}^-$. Further, a GARK method is called scalar L-stable if it is scalar A-stable,

$$\lim_{z^{\{f\}} \rightarrow \infty} R_1(z^{\{f\}}, z^{\{s\}}) = 0, \quad \text{and} \quad \lim_{z^{\{s\}} \rightarrow \infty} R_1(z^{\{f\}}, z^{\{s\}}) = 0. \quad (14)$$

Definition 2 (Scalar $A(\alpha)$ - and $L(\alpha)$ -stability). *A GARK method is scalar $A(\alpha)$ -stable if $S_1 \supseteq W(\alpha) \times W(\alpha)$, where $W(\alpha)$ is the wedge $\{z \in \mathbb{C} : |\arg(-z)| < \alpha, z \neq 0\}$. A scalar $A(\alpha)$ -stable GARK method that additionally satisfies eq. (14) is called scalar $L(\alpha)$ -stable.*

One way to determine if a single rate Runge–Kutta method is stable in the entire left half-plane is by ensuring stability on the imaginary axis and that the poles of $R(z)$ are in the right half-plane [11, Section IV.3]. Further, stability on the imaginary axis is equivalent to the E-polynomial

$$E(y) = Q(iy)Q(-iy) - P(iy)P(-iy)$$

being nonnegative for all $y \in \mathbb{R}$. Here, P and Q are the numerator and denominator of eq. (11), respectively. As we will now show, these practical techniques for determining stability have simple and direct generalizations for GARK methods applied to eq. (12).

Theorem 2 (Necessary and sufficient condition for scalar A-stability). *The GARK method eq. (3) is scalar A-stable if and only if*

$$\left| R_1(iy^{\{f\}}, iy^{\{s\}}) \right| \leq 1 \quad \text{for all } y^{\{f\}}, y^{\{s\}} \in \mathbb{R} \quad (15)$$

and R_1 is analytic over $\mathbb{C}^- \times \mathbb{C}^-$.

Proof. This follows from the multivariate maximum principle (see for example [26]). \square

Remark 1 (Finding $A(\alpha)$ -stability regions). *The maximum principle can also be used to efficiently determine the angle for scalar $A(\alpha)$ -stability. Instead of ensuring stability for all points inside a 4D wedge $W(\alpha) \times W(\alpha)$, one can limit the analysis to the boundary points $\partial W(\alpha) \times \partial W(\alpha)$.*

Notably, Theorem 2 reduces the space on which we have to check for A-stability from four to two dimensions. For multirate methods, however, R_1 is different for each value of M , thus adding another dimension to consider.

Theorem 3 (E-polynomial). *The E-polynomial for GARK methods is*

$$\begin{aligned} E_1(y^{\{f\}}, y^{\{s\}}) &= Q_1(iy^{\{f\}}, iy^{\{s\}}) Q_1(-iy^{\{f\}}, -iy^{\{s\}}) \\ &\quad - P_1(iy^{\{f\}}, iy^{\{s\}}) P_1(-iy^{\{f\}}, -iy^{\{s\}}), \end{aligned}$$

where P_1 and Q_1 are the numerator and denominator of eq. (13), respectively. The scalar stability region of a method contains the imaginary axes if and only if the E-polynomial is nonnegative for all $y^{\{f\}}, y^{\{s\}} \in \mathbb{R}$.

Proof. Following the single rate approach presented in [11, Section IV.3], we have that

$$\begin{aligned}
1 &\geq \left| R_1(i y^{\{f\}}, i y^{\{s\}}) \right|^2 \\
0 &\leq \left| Q_1(i y^{\{f\}}, i y^{\{s\}}) \right|^2 - \left| P_1(i y^{\{f\}}, i y^{\{s\}}) \right|^2 \\
0 &\leq Q_1(i y^{\{f\}}, i y^{\{s\}}) \overline{Q_1(i y^{\{f\}}, i y^{\{s\}})} - P_1(i y^{\{f\}}, i y^{\{s\}}) \overline{P_1(i y^{\{f\}}, i y^{\{s\}})} \\
0 &\leq Q_1(i y^{\{f\}}, i y^{\{s\}}) Q_1(-i y^{\{f\}}, -i y^{\{s\}}) - P_1(i y^{\{f\}}, i y^{\{s\}}) P_1(-i y^{\{f\}}, -i y^{\{s\}}) \\
0 &\leq E_1(y^{\{f\}}, y^{\{s\}}).
\end{aligned}$$

Since each of these inequalities is equivalent, the statement is proven. \square

3.2 2D test problem

Another test problem, first proposed in [6], and later used in [13, 24, 12, 4], is the 2D linear test problem

$$\begin{bmatrix} y^{\{f\}} \\ y^{\{s\}} \end{bmatrix}' = \underbrace{\begin{bmatrix} \lambda^{\{f\}} & \eta^{\{s\}} \\ \eta^{\{f\}} & \lambda^{\{s\}} \end{bmatrix}}_{\Lambda} \begin{bmatrix} y^{\{f\}} \\ y^{\{s\}} \end{bmatrix}. \quad (16)$$

Here, the exact solution must be bounded. That is, the eigenvalues of Λ have non-positive real parts and eigenvalues on the imaginary axis are regular. Further, we enforce that $\lambda^{\{f\}}, \lambda^{\{s\}} \in \mathbb{C}^-$ so the individual partitions have bounded dynamics. We will denote the set of these special exponentially bounded matrices by \mathbb{M} , and this test problem will be referred to as the complex 2D test problem. Many authors have considered simplifying assumptions including restricting Λ to real entries. In this case, the constraints on Λ simplify to $\lambda^{\{f\}}, \lambda^{\{s\}} \leq 0$, $\eta^{\{f\}} \eta^{\{s\}} \leq \lambda^{\{f\}} \lambda^{\{s\}}$, and a zero eigenvalue must be regular. We will refer to this problem as the real 2D test problem.

When eq. (3) is applied to eq. (16), we arrive at the stability matrix

$$\begin{aligned}
R_2 &\left(\begin{bmatrix} z^{\{f\}} & w^{\{s\}} \\ w^{\{f\}} & z^{\{s\}} \end{bmatrix} \right) \\
&= I_{2 \times 2} + \begin{bmatrix} \mathbf{b}^{\{f\}T} & 0 \\ 0 & \mathbf{b}^{\{s\}T} \end{bmatrix} \begin{bmatrix} I_{\mathbf{s}^{\{f\}} \times \mathbf{s}^{\{f\}}} - z^{\{f\}} \mathbf{A}^{\{f,f\}} & -w^{\{s\}} \mathbf{A}^{\{f,s\}} \\ -w^{\{f\}} \mathbf{A}^{\{s,f\}} & I_{\mathbf{s}^{\{s\}} \times \mathbf{s}^{\{s\}}} - z^{\{s\}} \mathbf{A}^{\{s,s\}} \end{bmatrix}^{-1} \quad (17) \\
&\quad \begin{bmatrix} z^{\{f\}} \mathbb{1}_{\mathbf{s}^{\{f\}}} & w^{\{s\}} \mathbb{1}_{\mathbf{s}^{\{f\}}} \\ w^{\{f\}} \mathbb{1}_{\mathbf{s}^{\{s\}}} & z^{\{s\}} \mathbb{1}_{\mathbf{s}^{\{s\}}} \end{bmatrix},
\end{aligned}$$

where

$$\begin{bmatrix} z^{\{f\}} & w^{\{s\}} \\ w^{\{f\}} & z^{\{s\}} \end{bmatrix} = H \begin{bmatrix} \lambda^{\{f\}} & \eta^{\{s\}} \\ \eta^{\{f\}} & \lambda^{\{s\}} \end{bmatrix}.$$

Definition 3 (Complex 2D region of absolute stability). *The set*

$$S_2 = \left\{ Z \in \mathbb{C}^{2 \times 2} : R_2(Z) \text{ power bounded} \right\}$$

is the complex 2D region of absolute stability for the test problem eq. (16). A GARK method is called complex 2D A-stable if $S_2 \supseteq \mathbb{M}$.

Definition 4 (Real 2D region of absolute stability). *The set*

$$\widehat{S}_2 = \left\{ Z \in \mathbb{R}^{2 \times 2} : R_2(Z) \text{ power bounded} \right\}$$

is the real 2D region of absolute stability for the test problem eq. (16). A GARK method is called real 2D A-stable if $\widehat{S}_2 \supseteq (\mathbb{M} \cap \mathbb{R}^{2 \times 2})$.

For both cases of the 2D test problem, the power boundedness condition makes finding necessary and sufficient conditions for stability significantly more challenging. Considering test problems on the boundary of \mathbb{M} does provide important necessary conditions. Consider the particular test problem

$$y' = \begin{bmatrix} 0 & \eta \\ -\eta & 0 \end{bmatrix} y, \quad (18)$$

which has purely imaginary eigenvalues for $\eta \in \mathbb{R}$. Note that

$$\begin{aligned} R_2 \left(\begin{bmatrix} 0 & w \\ -w & 0 \end{bmatrix} \right) &= I_{2 \times 2} + w \begin{bmatrix} \mathbf{b}^{\{f\}T} & 0 \\ 0 & \mathbf{b}^{\{s\}T} \end{bmatrix} \begin{bmatrix} I_{\mathbf{s}^{\{f\}} \times \mathbf{s}^{\{f\}}} & -w \mathbf{A}^{\{f,s\}} \\ w \mathbf{A}^{\{s,f\}} & I_{\mathbf{s}^{\{s\}} \times \mathbf{s}^{\{s\}}} \end{bmatrix}^{-1} \begin{bmatrix} 0 & \mathbb{1}_{\mathbf{s}^{\{f\}}} \\ -\mathbb{1}_{\mathbf{s}^{\{s\}}} & 0 \end{bmatrix} \\ &= \begin{bmatrix} 1 - w^2 \mathbf{b}^{\{f\}T} \mathbf{A}^{\{f,s\}} \mathbf{d}^{\{s\}} & w \mathbf{b}^{\{f\}T} \mathbf{d}^{\{f\}} \\ -w \mathbf{b}^{\{s\}T} \mathbf{d}^{\{s\}} & 1 - w^2 \mathbf{b}^{\{s\}T} \mathbf{A}^{\{s,f\}} \mathbf{d}^{\{f\}} \end{bmatrix}, \end{aligned} \quad (19)$$

where $w = H\eta$ and

$$\begin{aligned} \mathbf{d}^{\{f\}} &= \left(I_{\mathbf{s}^{\{f\}} \times \mathbf{s}^{\{f\}}} + w^2 \mathbf{A}^{\{f,s\}} \mathbf{A}^{\{s,f\}} \right)^{-1} \mathbb{1}_{\mathbf{s}^{\{f\}}}, \\ \mathbf{d}^{\{s\}} &= \left(I_{\mathbf{s}^{\{s\}} \times \mathbf{s}^{\{s\}}} + w^2 \mathbf{A}^{\{s,f\}} \mathbf{A}^{\{f,s\}} \right)^{-1} \mathbb{1}_{\mathbf{s}^{\{s\}}}. \end{aligned}$$

An important property of this stability function, which will be used later for theorem 5, is that it depends on the coupling coefficients but not the base method coefficients $A^{\{f,f\}}$ and $A^{\{s,s\}}$.

Remark 2 (Other test problems). *The 2D problem can be generalized to the linear block system*

$$\begin{bmatrix} y^{\{f\}} \\ y^{\{s\}} \end{bmatrix}' = \begin{bmatrix} \Lambda^{\{f\}} & E^{\{s\}} \\ E^{\{f\}} & \Lambda^{\{s\}} \end{bmatrix} \begin{bmatrix} y^{\{f\}} \\ y^{\{s\}} \end{bmatrix}. \quad (20)$$

This problem has been considered in [2, 7]. An even more general block system was used by Skelboe in [28]. We do not consider these block generalizations further as we find that the 2D problem already poses a surprisingly challenging test problem.

3.3 Comparison of stability test problems

When designing an implicit method, unconditional stability is a highly desirable property. A natural question is which test problem should be used to determine stability. In this section, we explore the relationships among the different stability criteria in order to address this question. Consider, for example, the GARK method given by the tableau below:

$$\begin{array}{c|c} 1 & 0 \\ \hline 1 & 1 \\ \hline 1 & 1 \end{array}$$

This method is scalar L-stable and even algebraically stable [22], but

$$\rho\left(R_2\left(\begin{bmatrix} -1 & 1 \\ -10 & -1 \end{bmatrix}\right)\right) = \frac{\sqrt{5}+3}{4} > 1,$$

with ρ the spectral radius operator. Thus, it is only conditionally stable for the real and complex 2D test problems.

Conversely, consider the GARK method

$$\begin{array}{c|cc} \frac{1}{4} & 0 & \frac{1}{4} \frac{1}{4} \\ \hline \frac{1}{4} & \frac{1}{4} & \frac{1}{4} \frac{1}{4} \\ \hline \frac{1}{4} & \frac{1}{4} & \frac{1}{4} 0 \\ \hline \frac{1}{4} & \frac{1}{4} & \frac{1}{4} \frac{1}{4} \\ \hline \frac{1}{2} & \frac{1}{2} & \frac{1}{2} \frac{1}{2} \end{array}$$

The base method is only $A(45^\circ)$ stable, and thus, it is easy to show the GARK method is conditionally stable with respect to the scalar test problem:

$$|R_1(-4 + 8i, 0)| = \frac{\sqrt{17}}{4} > 1. \quad (21)$$

For the real 2D test problem, this GARK method is A-stable. This result reveals a shortcoming of the real 2D test problem: the individual partitions have purely real eigenvalues. Ideally, a test problem should reveal instabilities of the base methods off the real axis. Despite the apparent independence of the stability functions eqs. (13) and (17), we do note that

$$R_1\left(z^{\{f\}}, z^{\{s\}}\right) = [z^{\{f\}} \ z^{\{s\}}] R_2\left(\begin{bmatrix} z^{\{f\}} & z^{\{s\}} \\ z^{\{f\}} & z^{\{s\}} \end{bmatrix}\right) \begin{bmatrix} \frac{\alpha}{z^{\{f\}}} \\ \frac{1-\alpha}{z^{\{s\}}} \end{bmatrix}, \quad (22a)$$

$$= [1 \ 1] R_2\left(\begin{bmatrix} z^{\{f\}} & z^{\{f\}} \\ z^{\{s\}} & z^{\{s\}} \end{bmatrix}\right) \begin{bmatrix} \alpha \\ 1-\alpha \end{bmatrix}, \quad (22b)$$

for any $\alpha \in \mathbb{C}$.

When eq. (16) is taken to have complex entries, however, there is a meaningful connection to the scalar test problem.

Theorem 4. *If a GARK method is A-stable with respect to the complex 2D test problem, then it is A-stable with respect to the scalar test problem.*

Proof. First, we define

$$R_2 \left(\begin{bmatrix} z^{\{f\}} & z^{\{f\}} \\ z^{\{s\}} & z^{\{s\}} \end{bmatrix} \right) = \begin{bmatrix} r_{1,1} & r_{1,2} \\ r_{2,1} & r_{2,2} \end{bmatrix}. \quad (23)$$

Since eq. (22b) must hold for all α ,

$$\text{const} = [1 \ 1] \begin{bmatrix} r_{1,1} & r_{1,2} \\ r_{2,1} & r_{2,2} \end{bmatrix} \begin{bmatrix} \alpha \\ 1 - \alpha \end{bmatrix} = \alpha(r_{1,1} + r_{2,1} - r_{1,2} - r_{2,2}) + r_{1,2} + r_{2,2}.$$

Thus, $r_{1,1} + r_{2,1} - r_{1,2} - r_{2,2} = 0$ and

$$R_2 \left(\begin{bmatrix} z^{\{f\}} & z^{\{f\}} \\ z^{\{s\}} & z^{\{s\}} \end{bmatrix} \right) = \begin{bmatrix} r_{1,1} & r_{1,2} \\ r_{2,1} & r_{1,1} + r_{2,1} - r_{1,2} \end{bmatrix}. \quad (24)$$

Due to this structure, the eigenvalues are simply $r_{1,1} \pm r_{1,2}$. If a GARK method is A-stable for the 2D test problem, then $|r_{1,1} + r_{2,1}| \leq 1$. Using eq. (22b) with $\alpha = 1$, we have that

$$\begin{aligned} R_1(z^{\{f\}}, z^{\{s\}}) &= [1 \ 1] R_2 \left(\begin{bmatrix} z^{\{f\}} & z^{\{f\}} \\ z^{\{s\}} & z^{\{s\}} \end{bmatrix} \right) \begin{bmatrix} 1 \\ 0 \end{bmatrix} \\ &= r_{1,1} + r_{2,1} \\ |R_1(z^{\{f\}}, z^{\{s\}})| &\leq 1. \end{aligned}$$

Thus, the method is A-stable for the scalar test problem. \square

While the 2D test problem may be a more thorough, reliable, and informative method of assessing stability, it is also more difficult to analyze and visualize due to the high-dimensional space of test problems. We summarize the hierarchy of linear stability properties in Figure 1.

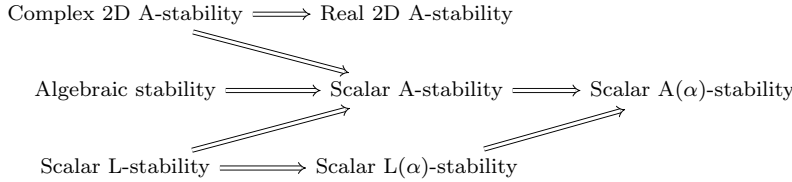


Fig. 1 Stability implications for the various linear test problems. In general, no implication arrows are reversible.

Lemma 1. *For a decoupled GARK method, the following matrix is nilpotent:*

$$\begin{bmatrix} 0 & \mathbf{A}^{\{f,s\}} \\ \mathbf{A}^{\{s,f\}} & 0 \end{bmatrix}.$$

Proof. The full matrix \mathbf{A} can be viewed as the adjacency matrix of a weighted directed graph. Cycles indicate the method is implicit, and by the definition of a decoupled method, implicitness only comes from the base methods. With the base method coefficients set to zero, the directed graph becomes acyclic: a property equivalent to nilpotency of the adjacency matrix. \square

Theorem 5. *A decoupled GARK method consistent with eq. (1) (first order accurate) cannot be A-stable for the real 2D test problem.*

Proof. Consider the particular test problem given in eq. (18). Note that in eq. (19), the matrix being inverted is the sum of an identity matrix and a nilpotent matrix by the decoupled assumption and lemma 1. Expanding the inverse in a Neumann series reveals $\mathbf{d}^{\{f\}}$ and $\mathbf{d}^{\{s\}}$ must be even polynomials in w of finite degree. Moreover, the off-diagonal terms of the stability matrix satisfy

$$w \mathbf{b}^{\{f\}T} \mathbf{d}^{\{f\}} = w \mathbf{b}^{\{f\}T} \left(I + w^2 \mathbf{A}^{\{f,s\}} \mathbf{A}^{\{s,f\}} + \dots \right) \mathbf{1}_{\mathbf{s}^{\{f\}}} = w + w^3 p_{1,2}(w^2),$$

$$-w \mathbf{b}^{\{s\}T} \mathbf{d}^{\{s\}} = -w \mathbf{b}^{\{s\}T} \left(I + w^2 \mathbf{A}^{\{s,f\}} \mathbf{A}^{\{f,s\}} + \dots \right) \mathbf{1}_{\mathbf{s}^{\{s\}}} = -w - w^3 p_{2,1}(w^2),$$

where $p_{1,2}$ and $p_{2,1}$ are polynomials. Note the consistency assumption implies $\mathbf{b}^{\{f\}T} \mathbf{1}_{\mathbf{s}^{\{f\}}} = \mathbf{b}^{\{s\}T} \mathbf{1}_{\mathbf{s}^{\{s\}}} = 1$ and is used to determine the coefficient multiplying the w terms. Now the stability matrix can be written in the form

$$R_2(w) = \begin{bmatrix} 1 - w^2 p_{1,1}(w^2) & w + w^3 p_{1,2}(w^2) \\ -w - w^3 p_{2,1}(w^2) & 1 - w^2 p_{2,2}(w^2) \end{bmatrix},$$

where $p_{1,1}$, and $p_{2,2}$ are also polynomials.

Suppose by means of contradiction that the method is A-stable. Consider the trace of the stability matrix:

$$\text{tr}(R_2(w)) = 2 - w^2 (p_{1,1}(w^2) + p_{2,2}(w^2)).$$

In order to avoid an eigenvalue of $R_2(w)$ being unbounded in w , we must have that $p_{2,2}(w^2) = -p_{1,1}(w^2)$. Using this necessary condition, the determinant is

$$\begin{aligned} \det(R_2(w)) &= (1 - w^2 p_{1,1}(w^2))(1 + w^2 p_{1,1}(w^2)) \\ &\quad - (w + w^3 p_{1,2}(w^2))(-w - w^3 p_{2,1}(w^2)) \\ &= 1 + w^2 + \mathcal{O}(w^4). \end{aligned}$$

Since the determinant grows unbounded in w , the spectral radius can be made arbitrarily large. This is a contradiction. Therefore, the method cannot be A-stable for the real 2D test problem. \square

3.4 Compound-step stability

Directly using the general stability formula eq. (13) on an MrGARK method requires inverting a matrix of size $\mathbf{s} \times \mathbf{s}$. When trying to analyze or visualize the linear stability for large M , this becomes very expensive. Fortunately, the particular structure of compound-step MrGARK methods allows for an explicit derivation of the scalar stability function using only matrices of size $s \times s$.

For the base method (A, b, c) , let $R_{\text{int}}(z)$ be the internal stability function:

$$R_{\text{int}}(z) = (I_{s \times s} - z A)^{-1} \mathbf{1}_s.$$

We now seek to find the scalar internal stability of a compound-step MrGARK method. Let $z = z^{\{\mathfrak{f}\}} + z^{\{\mathfrak{s}\}}$. Then the first macro-step eq. (8a) is composed of traditional Runge–Kutta stages and is simply

$$Y = y_n R_{\text{int}}(z) \quad (25)$$

for the scalar linear test problem. The λ -th fast micro-step eq. (8b) has stages defined by the recurrence relation

$$Y^{\{\mathfrak{f},\lambda\}} = y_n \mathbb{1}_s + \frac{z^{\{\mathfrak{f}\}}}{M} \sum_{k=1}^{\lambda-1} \mathbb{1}_s b^T Y^{\{\mathfrak{f},k\}} + \frac{z^{\{\mathfrak{f}\}}}{M} A Y^{\{\mathfrak{f},\lambda\}} + z^{\{\mathfrak{s}\}} A^{\{\mathfrak{f},\mathfrak{s},\lambda\}} Y.$$

Solving for $Y^{\{\mathfrak{f},\lambda\}}$ explicitly is equivalent to solving the following linear system via block backwards substitution:

$$\begin{bmatrix} I - \frac{z^{\{\mathfrak{f}\}}}{M} A & \dots & 0 \\ \vdots & \ddots & \vdots \\ -\frac{z^{\{\mathfrak{f}\}}}{M} \mathbb{1}_s b^T & \dots & I - \frac{z^{\{\mathfrak{f}\}}}{M} A \end{bmatrix} \begin{bmatrix} Y^{\{\mathfrak{f},1\}} \\ \vdots \\ Y^{\{\mathfrak{f},M\}} \end{bmatrix} = \begin{bmatrix} y_n \mathbb{1}_s + z^{\{\mathfrak{s}\}} A^{\{\mathfrak{f},\mathfrak{s},1\}} Y \\ \vdots \\ y_n \mathbb{1}_s + z^{\{\mathfrak{s}\}} A^{\{\mathfrak{f},\mathfrak{s},M\}} Y \end{bmatrix}.$$

This yields

$$\begin{aligned} Y^{\{\mathfrak{f},\lambda\}} &= \frac{z^{\{\mathfrak{f}\}}}{M} R_{\text{int}}\left(\frac{z^{\{\mathfrak{f}\}}}{M}\right) b^T \left(I - \frac{z^{\{\mathfrak{f}\}}}{M} A\right)^{-1} \sum_{k=1}^{\lambda-1} R\left(\frac{z^{\{\mathfrak{f}\}}}{M}\right)^{\lambda-1-k} (y_n \mathbb{1}_s \\ &\quad + z^{\{\mathfrak{s}\}} A^{\{\mathfrak{f},\mathfrak{s},k\}} Y) + \left(I - \frac{z^{\{\mathfrak{f}\}}}{M} A\right)^{-1} (y_n \mathbb{1}_s + z^{\{\mathfrak{s}\}} A^{\{\mathfrak{f},\mathfrak{s},\lambda\}} Y) \\ &= \left(\frac{z^{\{\mathfrak{f}\}} z^{\{\mathfrak{s}\}}}{M} R_{\text{int}}\left(\frac{z^{\{\mathfrak{f}\}}}{M}\right) b^T \left(I - \frac{z^{\{\mathfrak{f}\}}}{M} A\right)^{-1} \sum_{k=1}^{\lambda-1} R\left(\frac{z^{\{\mathfrak{f}\}}}{M}\right)^{\lambda-1-k} A^{\{\mathfrak{f},\mathfrak{s},k\}} R_{\text{int}}(z)\right. \\ &\quad \left. + z^{\{\mathfrak{s}\}} \left(I - \frac{z^{\{\mathfrak{f}\}}}{M} A\right)^{-1} A^{\{\mathfrak{f},\mathfrak{s},\lambda\}} R_{\text{int}}(z) + R\left(\frac{z^{\{\mathfrak{f}\}}}{M}\right)^{\lambda-1} R_{\text{int}}\left(\frac{z^{\{\mathfrak{f}\}}}{M}\right)\right) y_n. \end{aligned} \quad (26)$$

Together, eqs. (25) and (26) form the internal stability for a compound-step MrGARK method. With this in hand, the scalar linear stability function eq. (13) can be derived:

$$\begin{aligned} R_1(z^{\{\mathfrak{f}\}}, z^{\{\mathfrak{s}\}}) &= 1 + \frac{z^{\{\mathfrak{f}\}}}{M} \sum_{\lambda=1}^M b^T Y^{\{\mathfrak{f},\mathfrak{s},\lambda\}} + z^{\{\mathfrak{s}\}} b^T Y \\ &= R\left(\frac{z^{\{\mathfrak{f}\}}}{M}\right)^M + z^{\{\mathfrak{s}\}} b^T R_{\text{int}}(z) \\ &\quad + \frac{z^{\{\mathfrak{s}\}} z^{\{\mathfrak{f}\}}}{M} b^T \left(I_{s \times s} - \frac{z^{\{\mathfrak{f}\}}}{M} A\right)^{-1} \sum_{\lambda=1}^M R\left(\frac{z^{\{\mathfrak{f}\}}}{M}\right)^{M-\lambda} A^{\{\mathfrak{f},\mathfrak{s},\lambda\}} R_{\text{int}}(z). \end{aligned}$$

If A is invertible, then $R_{\text{int}}(-\infty) = 0_s$ and

$$\begin{aligned} \lim_{z^{\{\mathfrak{f}\}} \rightarrow -\infty} R_1(z^{\{\mathfrak{f}\}}, z^{\{\mathfrak{s}\}}) &= R(-\infty)^M + z^{\{\mathfrak{s}\}} \left(b^T - b^T A^{-1} A^{\{\mathfrak{f}, \mathfrak{s}, M\}} \right) R_{\text{int}}(-\infty) \\ &= R(-\infty)^M. \end{aligned}$$

The other limit is more difficult to approach directly, so we consider first the internal stability eq. (26). Starting with the first micro-step, we have that

$$\lim_{z^{\{\mathfrak{s}\}} \rightarrow -\infty} Y^{\{\mathfrak{f}, 1\}} = \left(I - \frac{z^{\{\mathfrak{f}\}}}{M} A \right)^{-1} \left(\mathbb{1}_s - A^{\{\mathfrak{f}, \mathfrak{s}, 1\}} A^{-1} \mathbb{1}_s \right) y_n.$$

This suggests the condition $A^{\{\mathfrak{f}, \mathfrak{s}, 1\}} A^{-1} \mathbb{1}_s = \mathbb{1}_s$ to ensure the stage values go to zero in the limit. Now we can use an inductive argument to generalize this condition for the remaining micro-step stages. Assume that $\lim_{z^{\{\mathfrak{s}\}} \rightarrow -\infty} Y^{\{\mathfrak{f}, \ell\}} = 0$ for $\ell = 1, \dots, \lambda - 1$. Then

$$\lim_{z^{\{\mathfrak{s}\}} \rightarrow -\infty} Y^{\{\mathfrak{f}, \lambda\}} = \left(I_{s \times s} - \frac{z^{\{\mathfrak{f}\}}}{M} A \right)^{-1} \left(\mathbb{1}_s - A^{\{\mathfrak{f}, \mathfrak{s}, \lambda\}} A^{-1} \mathbb{1}_s \right) y_n.$$

This suggests the condition

$$A^{\{\mathfrak{f}, \mathfrak{s}, \lambda\}} A^{-1} \mathbb{1}_s = \mathbb{1}_s, \quad \lambda = 1, \dots, M \quad (27)$$

to ensure all stages go to zero in the limit. Further eq. (27) leads to the result

$$\lim_{z^{\{\mathfrak{s}\}} \rightarrow -\infty} R_1(z^{\{\mathfrak{f}\}}, z^{\{\mathfrak{s}\}}) = R(-\infty) + \frac{z^{\{\mathfrak{f}\}}}{M} \sum_{\lambda=1}^M b^T Y^{\{\mathfrak{f}, \mathfrak{s}, \lambda\}} = R(-\infty).$$

4 Numerical solution of implicit stage equations

The key to an efficient implicit GARK method is an efficient Newton iteration. Written compactly, the stage equations are

$$\widehat{Y} = \mathbb{1}_s \otimes y_n + H(\mathbf{A} \otimes I_{d \times d}) \widehat{f}(\widehat{Y}), \quad (28)$$

where

$$\widehat{Y} = \begin{bmatrix} Y^{\{\mathfrak{f}\}} \\ Y^{\{\mathfrak{s}\}} \end{bmatrix}, \quad \widehat{f}(\widehat{Y}) = \begin{bmatrix} f^{\{\mathfrak{f}\}}(Y^{\{\mathfrak{f}\}}) \\ f^{\{\mathfrak{s}\}}(Y^{\{\mathfrak{s}\}}) \end{bmatrix}. \quad (29)$$

Applying Newton's method to solve for the stages yields the iterative procedure

$$(I_{s \times s} \otimes I_{d \times d} - H(\mathbf{A} \otimes I_{d \times d}) \widehat{J}) \delta = -\widehat{Y} + \mathbb{1}_s \otimes y_n + H(\mathbf{A} \otimes I_{d \times d}) \widehat{f}(\widehat{Y}), \quad (30a)$$

$$\widehat{Y} = \widehat{Y} + \delta, \quad (30b)$$

with

$$\widehat{J} = \text{diag} \left(J_1^{\{\mathfrak{f}\}}, \dots, J_{s^{\{\mathfrak{f}\}}}^{\{\mathfrak{f}\}}, J_1^{\{\mathfrak{s}\}}, \dots, J_{s^{\{\mathfrak{s}\}}}^{\{\mathfrak{s}\}} \right), \quad (31)$$

and $J_i^{\{\sigma\}} = \frac{\partial f^{\{\sigma\}}}{\partial y} \left(Y_i^{\{\sigma\}} \right)$ for $\sigma \in \{\mathfrak{s}, \mathfrak{f}\}$.

In single rate Newton iterations, it is common to evaluate the Jacobian once at y_n and use it across all stages which yields a cheaper modified Newton's method. A similar strategy can be employed for each partition's Jacobian in a GARK Newton iteration. For multirate methods, it might be beneficial to reevaluate the fast Jacobian at each micro-step and keep the slow Jacobian across the entire macro-step.

We note that eq. (30) serves mostly theoretical purposes, as it is impractically expensive and rarely necessary to simultaneously solve for all s stages. All methods presented in section 5, for example, require solving nonlinear systems with dimension no larger than d . In this section, we will explore techniques and method structures that allow for these efficient implementations of Newton iterations. In the cost analyses we present, matrix decompositions involving the Jacobians are assumed to be the dominant cost of a step.

4.1 Decoupled methods

As described in section 2.1, decoupled methods only have implicitness in the base methods. For this subsection, we will assume both base methods are diagonally implicit which seems to be the most practical structure for decoupled implicit methods. Now, each of the s method stages defines a d -dimensional nonlinear equation which can be solved sequentially for a cost of $\mathcal{O}(s d^3)$, assuming direct methods are used. If we further assume the slow matrix decomposition is reused across a multirate macro-step and the fast matrix decomposition is reused across a micro-step, the cost is reduced to $\mathcal{O}(M d^3)$. It is important to note that the slow and fast Jacobians are likely to have simpler structures than the full Jacobian, and these structures can be exploited in the linear solves.

For the special case of component partitioned systems eq. (2), the linear solves are of the reduced dimensions $d^{\{f\}}$ and $d^{\{s\}}$. In the most extreme case where each variable of a system forms a partition, a step would involve scalar Newton iterations for all variables and only the diagonal of the Jacobian of f would be required. We note, however, that this leads to an explosion in the number of coupling error terms and degraded stability.

4.2 Compound-step methods

Compound-step methods start by taking a full macro-step like a single rate Runge–Kutta method. Consequently, the nonlinear equations for the stages can be solved just as they would for a single rate method. When using Newton's method, the full, unpartitioned Jacobian is used. It may be appropriate to loosen the solver tolerances of the fast variables for the compound step as they will be recomputed later [30]. Although the remaining micro-steps are also implicitly defined, only $J_i^{\{f\}}$ is now involved in Newton iterations. Assuming a diagonally implicit structure for

the base method, these Newton iterations are of the form

$$\begin{aligned} \left(I_{d \times d} - h a_{i,i}^{\{\mathfrak{f},\mathfrak{f}\}} J_i^{\{\mathfrak{f}\}} \right) \delta &= -Y_i^{\{\mathfrak{f},\lambda\}} + \tilde{y}_{n+(\lambda-1)/M} + h \sum_{j=1}^{s^{\{\mathfrak{f}\}}} a_{i,j}^{\{\mathfrak{f},\mathfrak{f}\}} f^{\{\mathfrak{f}\}}(Y_j^{\{\mathfrak{f},\lambda\}}) \\ &+ H \sum_{j=1}^{s^{\{\mathfrak{s}\}}} a_{i,j}^{\{\mathfrak{f},\mathfrak{s},\lambda\}} f^{\{\mathfrak{s}\}}(Y_j). \end{aligned}$$

We note that an accurate stage value predictor to determine an initial δ can come from dense output of the compound step.

In an implementation where a decomposition of the full matrix is formed once and a decomposition for the fast matrix is formed at each micro-step, the total cost for one step is $\mathcal{O}(M d^3)$. For component partitioned systems, this reduces to $\mathcal{O}(d^3 + M d^{\{\mathfrak{f}\}} \times 3)$.

4.3 Stage reducibility

Consider the simple methods defined by the GARK tableaus eq. (4) below:

$$\begin{array}{c|c} 1 & 1 \\ \hline 1 & 1 \end{array} \quad \text{and} \quad \begin{array}{c|c} \frac{1}{2} & 1 \\ \hline \frac{1}{2} & 1 \\ \hline 1 & 1 \end{array}.$$

The former is backward Euler cast into the GARK framework. A direct application of eq. (30) would require solving linear systems of size $2d$ when clearly solves of size d can suffice. Here, $Y_1^{\{\mathfrak{f}\}} = Y_1^{\{\mathfrak{s}\}}$, and these stages fall back onto the traditional backward Euler stage $Y_1 = y_n + H f(Y_1)$. The latter method, which is an additive Runge–Kutta (ARK) method cast into the GARK framework, also has $Y_1^{\{\mathfrak{f}\}} = Y_1^{\{\mathfrak{s}\}}$. Equation (30a) can be simplified to

$$\left(I_{d \times d} - \frac{H}{2} J_1^{\{\mathfrak{f}\}} + H J_1^{\{\mathfrak{s}\}} \right) \delta = -Y_1 + y_n + \frac{H}{2} f^{\{\mathfrak{f}\}}(Y_1) + H f^{\{\mathfrak{s}\}}(Y_1). \quad (32)$$

More generally when a row of GARK coefficients is repeated in multiple partitions, the number of unknowns in eq. (28) and the dimension of the Newton iteration is reduced. We call this *stage reducibility*. Compound-step methods, for example, have this property in the first s stages.

In Section 5, we develop new multirate coupling strategies that utilize this simplification. An interesting property is that the solves involve matrices of the form $I_{d \times d} - h \gamma J_i^{\{\mathfrak{f}\}} - H \gamma J_i^{\{\mathfrak{s}\}}$. Note $J_i^{\{\mathfrak{f}\}}$ is scaled by the micro-step, while $J_i^{\{\mathfrak{s}\}}$ is scaled by the macro-step. If the multirate ratio is based on partition stiffness, then the scaled matrices should have similar spectral radii. By damping the fast, stiff modes, the conditioning of this system can be much better than the traditional $I_{d \times d} - H \gamma J_i$.

4.4 Low rank structure of matrices in Newton iteration

When a GARK method has stage reducibility, \mathbf{A} cannot be full rank due to at least one repeated row. An alternative simplification arises by applying the Woodbury matrix identity to reduce the dimension of the linear solve. Using the GARK method below, we demonstrate that this idea can be extended to a broader set of schemes:

$$\begin{array}{c|c} \frac{1}{2} & \frac{1}{2} \\ \hline 1 & 1 \\ \hline 1 & 1 \end{array}.$$

We have the following simplification in the Newton iteration:

$$\begin{aligned} & \left(I_{s \times s} \otimes I_{d \times d} - H (\mathbf{A} \otimes I_{d \times d}) \hat{J} \right)^{-1} \\ &= \left(\begin{bmatrix} I_{d \times d} & 0 \\ 0 & I_{d \times d} \end{bmatrix} - H \begin{bmatrix} \frac{1}{2} J_1^{\{f\}} & \frac{1}{2} J_1^{\{s\}} \\ J_1^{\{f\}} & J_1^{\{s\}} \end{bmatrix} \right)^{-1} \\ &= \begin{bmatrix} I_{d \times d} & 0 \\ 0 & I_{d \times d} \end{bmatrix} + \begin{bmatrix} \frac{H}{2} I_{d \times d} \\ H I_{d \times d} \end{bmatrix} \left(I_{d \times d} - \frac{H}{2} J_1^{\{f\}} - H J_1^{\{s\}} \right)^{-1} \begin{bmatrix} J_1^{\{f\}} & J_1^{\{s\}} \end{bmatrix}. \end{aligned}$$

Compared to eq. (32), additional matrix-vector products are required, but ultimately, the same matrix inverse appears. Thus, the potential to have improved conditioning is still present.

5 Practical implicit MrGARK methods

In this section, we present new methods of orders one to four. At high order, coupling coefficients can become complicated rational functions of λ and M . In addition to listing the coefficients in this paper, a Mathematica notebook with the coefficients is provided in the supplementary materials to aid those implementing the methods.

5.1 First order

Multirate methods of order one have no coupling conditions which allows a great amount of freedom in deriving coefficients, but for implicit methods, stability does impose some important constraints. Theorem 6 eliminates one subset of first order methods from being scalar A-stable.

Theorem 6. *An internally consistent MrGARK method of order exactly one is only scalar A-stable for a finite number of multirate ratios.*

Proof. Using the internal consistency assumptions, the magnitude of the scalar stability function can be expanded as

$$\begin{aligned}
|R_1(i\omega^{\{f\}}y, i\omega^{\{s\}}y)|^2 &= 1 + y^2 \left(\omega^{\{f\}} + \omega^{\{s\}} \right)^2 \\
&\quad - 2y^2 \left(\left(\omega^{\{f\}} + \omega^{\{s\}} \right) \left(\omega^{\{f\}} \mathbf{b}^{\{f\}T} \mathbf{c}^{\{f\}} + \omega^{\{s\}} \mathbf{b}^{\{s\}T} \mathbf{c}^{\{s\}} \right) \right) \\
&\quad + \mathcal{O}(y^4) \\
&= 1 + y^2 p(\omega^{\{f\}}, \omega^{\{s\}}) + \mathcal{O}(y^4).
\end{aligned} \tag{33}$$

Let H be the Hessian matrix of the homogeneous polynomial of degree two p . Note that $\det(H) = -4 \left(r^{\{f\}} - r^{\{s\}} \right)^2$, where $r^{\{f\}} = \mathbf{b}^{\{f\}T} \mathbf{c}^{\{f\}} - \frac{1}{2}$ and $r^{\{s\}} = \mathbf{b}^{\{s\}T} \mathbf{c}^{\{s\}} - \frac{1}{2}$ which are the second order residuals. These residuals cannot both be zero because the GARK method would be order two by internal consistency. When one base method is order one and the other is higher order, these residuals must differ. Otherwise, when both base methods have order one, $r^{\{f\}}$ is a function of M which approaches zero while $r^{\{s\}}$ is a fixed nonzero constant. For all but a finite set of M , these residuals must differ. Whenever the residuals differ, p is saddle-shaped, and there exist $\omega^{\{f\}}$ and $\omega^{\{s\}}$ such that the polynomial is positive. For sufficiently small values of y , the positive $y^2 p(\omega^{\{f\}}, \omega^{\{s\}})$ term will dominate the $\mathcal{O}(y^4)$ term in eq. (33). Thus, for all but a finite set of M , there are $\omega^{\{f\}}$, $\omega^{\{s\}}$, and y such that $|R_1(i\omega^{\{f\}}y, i\omega^{\{s\}}y)| > 1$. \square

Remark 3. Note that theorem 6 imposes no restriction on the multirate strategy. It only requires the defining characteristic of a multirate method: the fast error asymptotically approaches zero as M increases.

At first order, the natural choice for an implicit base method is backward Euler. There is currently a plethora of multirate backward Euler schemes in the literature (see [20, 31, 33, 10]). These schemes feature nearly all the different combinations of coupled or decoupled, internal consistency or internal inconsistency, and parallel or sequential methods. In the search for a multirate backward Euler method with excellent stability and accuracy properties, we developed the coupling strategy given by the following coupling coefficients:

$$A^{\{f,s,\lambda\}} = \begin{bmatrix} 0 & \lambda < \frac{M}{2} \\ 1 & \text{otherwise} \end{bmatrix}, \quad A^{\{s,f,\lambda\}} = \begin{bmatrix} 1 & \lambda \leq \frac{M+1}{2} \\ 0 & \text{otherwise} \end{bmatrix}. \tag{34}$$

This method has one coupled stage, but with stage reducibility (section 4.3), and all other stages are decoupled. Further, it is internally inconsistent and is scalar L- and algebraically stable for all M . A decoupled counterpart is given by the following coupling coefficients:

$$A^{\{f,s,\lambda\}} = \begin{bmatrix} 0 & \lambda \leq \frac{M}{2} \\ 1 & \text{otherwise} \end{bmatrix}, \quad A^{\{s,f,\lambda\}} = \begin{bmatrix} 1 & \lambda \leq \frac{M}{2} \\ 0 & \text{otherwise} \end{bmatrix}. \tag{35}$$

This method is internally inconsistent, has no second order coupling error when M is even, and is scalar L- and algebraically stable for all M .

We note this method is closely connected to the following subcycled Strang splitting [29]:

$$\varphi_H^f = \left(\varphi_h^{f\{\mathfrak{f}\}} \right)^{M/2} \circ \varphi_H^{f\{\mathfrak{s}\}} \circ \left(\varphi_h^{f\{\mathfrak{f}\}} \right)^{M/2} + \mathcal{O}(H^2).$$

Here, the operator φ_t^g maps an initial condition for the ODE $y' = g(y)$ to the solution at time t . If we approximate these exact ODE solutions with one step of the backward Euler method, we recover the decoupled multirate backward Euler scheme eq. (35).

5.2 Second order

The simplest second order base method is the one stage implicit midpoint method:

$$\begin{array}{c|c} \frac{1}{2} & \frac{1}{2} \\ \hline & 1 \end{array}$$

The standard MrGARK coupling coefficients

$$A^{\{\mathfrak{f}, \mathfrak{s}, \lambda\}} = \begin{bmatrix} 0 & \lambda < L \\ \frac{1}{2} & \lambda = L \\ 1 & \lambda > L \end{bmatrix}, \quad A^{\{\mathfrak{s}, \mathfrak{f}, \lambda\}} = \begin{bmatrix} 1 & \lambda < L \\ \frac{1}{2} & \lambda = L \\ 0 & \lambda > L \end{bmatrix},$$

for odd M and $L = \frac{M+1}{2}$ give a coupled multirate midpoint method. Similar to the coupled backward Euler method eq. (34), one stage is coupled but with stage reducibility, and all other stages are decoupled. Reusing the coupling coefficients eq. (35) with even M and the midpoint method as the base, we derive a decoupled multirate midpoint method. Notably, both schemes maintain the algebraic stability, symmetry, and symplecticity of the midpoint method. With only odd order terms appearing in the error expansion, they can be used to build efficient multirate extrapolation methods.

We also consider the L-stable, order two SDIRK base method from [1]

$$\begin{array}{c|cc} \gamma & \gamma & 0 \\ \hline 1 & 1 - \gamma & \gamma \\ \hline & 1 - \gamma & \gamma \\ \hline & \frac{3}{5} & \frac{2}{5} \end{array}$$

with $\gamma = 1 - 1/\sqrt{2}$. For this base method, an internally consistent standard MrGARK method must have at least one coupled stage. Enforcing stiff accuracy for

both partitions uniquely determines a lightly coupled method:

$$A^{\{\mathfrak{f}, \mathfrak{s}, \lambda\}} = \begin{bmatrix} \frac{\lambda-1+\gamma}{M} & 0 \\ \begin{cases} 1-\gamma & \lambda = M \\ \frac{\lambda}{M} & \text{otherwise} \end{cases} & \begin{cases} \gamma & \lambda = M \\ 0 & \text{otherwise} \end{cases} \end{bmatrix},$$

$$A^{\{\mathfrak{s}, \mathfrak{f}, \lambda\}} = \begin{bmatrix} M\gamma & \lambda = 1 & 0 \\ 0 & \text{otherwise} & 1-\gamma \\ 1-\gamma & & \gamma \end{bmatrix}.$$

For this method, the first slow and fast stages are coupled, but with low rank structure. The last slow and fast stages are also coupled, but with stage reducibility. All other stages are decoupled. Another coupling strategy is that of Kværnø and Rentrop [14, 9] in which the first micro-step and the macro-step are computed together. The following coupling coefficients take this approach and also enforces eq. (14):

$$A^{\{\mathfrak{f}, \mathfrak{s}, \lambda\}} = \begin{bmatrix} \frac{\gamma(2\lambda-1)}{M} & \begin{cases} 0 & \lambda = 1 \\ \frac{(\lambda-1)(1-2\gamma)}{M} & \lambda > 1 \end{cases} \\ \frac{1-3\gamma+2\gamma\lambda}{M} & \frac{3\gamma-1+(1-2\gamma)\lambda}{M} \end{bmatrix},$$

$$A^{\{\mathfrak{s}, \mathfrak{f}, \lambda\}} = \begin{cases} M \begin{bmatrix} \gamma & 0 \\ 1-\gamma & \gamma \end{bmatrix} & \lambda = 1 \\ 0_{2 \times 2} & \text{otherwise} \end{cases}.$$

Here, the first two fast and slow stages are coupled, but with low rank structure.

An interesting feature of these two coupled methods is they have identical stability functions for all M . Unfortunately as M increases, instabilities appear near the origin. At $M = 2$, the methods are only scalar $L(69.2^\circ)$ -stable (as defined in definition 2), and by $M = 6$ they are not even scalar $L(0^\circ)$ -stable. This is a surprising result as these seemingly reasonable coupling structures lead to methods with worse stability and a more expensive implementation than the decoupled multirate midpoint method. As is the case with order one, it appears that internal consistency negatively affects the stability.

The following compound-step method, which we will call compounds-step MrGARK SDIRK 2, can be derived from stability condition eq. (27) and internal consistency:

$$A^{\{\mathfrak{f}, \mathfrak{s}, \lambda\}} = \begin{bmatrix} \frac{-\gamma((M-2)\gamma+3)+(2\gamma-1)\lambda+1}{M(\gamma-1)} & \frac{\gamma((M-1)\gamma-\lambda+1)}{M(\gamma-1)} \\ \frac{M\gamma^2-2\lambda\gamma+\lambda}{M-M\gamma} & \frac{\gamma(M\gamma-\lambda)}{M(\gamma-1)} \end{bmatrix}. \quad (36)$$

The angles of $L(\alpha)$ -stability for several values of M are listed in table 1. Unlike the aforementioned internally consistent methods of order two, compounds-step MrGARK SDIRK 2 maintains a wide angle when M is large.

5.3 Third order

A third order compound-step method, which we will refer to as compound-step MrGARK SDIRK 3, is built on the following L-stable base method of Alexander

[1]:

$$\begin{array}{c|cccc}
 \gamma & \gamma & 0 & 0 \\
 \hline
 \frac{\gamma}{2} + \frac{1}{2} & \frac{1}{2} - \frac{\gamma}{2} & \gamma & 0 \\
 \hline
 1 & -\frac{3\gamma^2}{2} + 4\gamma - \frac{1}{4} & \frac{3\gamma^2}{2} - 5\gamma + \frac{5}{4} & \gamma \\
 \hline
 -\frac{3\gamma^2}{2} + 4\gamma - \frac{1}{4} & \frac{3\gamma^2}{2} - 5\gamma + \frac{5}{4} & \gamma \\
 \hline
 -\frac{3\gamma^2}{2} + 3\gamma - \frac{1}{4} & \frac{3\gamma^2}{2} - 3\gamma + \frac{5}{4} & 0
 \end{array}$$

$$\gamma = 1 - \frac{\cos\left(\frac{1}{3}\cot^{-1}(2\sqrt{2})\right)}{\sqrt{2}} + \sqrt{\frac{3}{2}}\sin\left(\frac{1}{3}\cot^{-1}(2\sqrt{2})\right) \approx 0.4358665215084590.$$

The coupling coefficients were derived such as to be bounded functions of λ and M , as well as to satisfy eq. (27):

$$\begin{aligned}
 a_{1,1}^{\{\mathfrak{f}, \mathfrak{s}, \lambda\}} &= \frac{(6\gamma^2 - 24\gamma + 5)(2\gamma^2 + 2\gamma(\lambda - 1) + (\lambda - 1)^2) - 8\gamma^3 M^2 - (6\gamma^3 - 30\gamma^2 - 15\gamma + 5)M(\gamma + \lambda - 1)}{(\gamma - 1)(6\gamma^2 - 20\gamma + 5)M^2}, \\
 a_{1,2}^{\{\mathfrak{f}, \mathfrak{s}, \lambda\}} &= \frac{-5(\lambda - 1)^2 + 12\gamma^4(M - 1) + 4\gamma^3(M - 1)(3\lambda + 4M - 17)}{(\gamma - 1)(6\gamma^2 - 20\gamma + 5)M^2} \\
 &\quad + \frac{\gamma^2(-6\lambda^2 + 68\lambda + (82 - 72\lambda)M - 72) + 2\gamma(\lambda - 1)(14\lambda + 5M - 19)}{(\gamma - 1)(6\gamma^2 - 20\gamma + 5)M^2}, \\
 a_{1,3}^{\{\mathfrak{f}, \mathfrak{s}, \lambda\}} &= -\frac{4\gamma((\lambda - 1)^2 + 2\gamma^2(M - 1)^2 - 2\gamma(\lambda - 1)(2M - 1))}{(\gamma - 1)(6\gamma^2 - 20\gamma + 5)M^2}, \\
 a_{2,1}^{\{\mathfrak{f}, \mathfrak{s}, \lambda\}} &= -\frac{-2(6\gamma^2 - 24\gamma + 5)(\gamma(\lambda + 1) + (\lambda - 1)\lambda) + 16\gamma^3 M^2 + (6\gamma^3 - 30\gamma^2 - 15\gamma + 5)M(\gamma + 2\lambda - 1)}{2(\gamma - 1)(6\gamma^2 - 20\gamma + 5)M^2}, \\
 a_{2,2}^{\{\mathfrak{f}, \mathfrak{s}, \lambda\}} &= \frac{-5(\lambda - 1)\lambda + 2\gamma^3(-3(\lambda + 1) + 8M^2 + 3(2\lambda - 7)M)}{(\gamma - 1)(6\gamma^2 - 20\gamma + 5)M^2} \\
 &\quad + \frac{6\gamma^4 M + \gamma^2(-6\lambda^2 + 34\lambda + (41 - 72\lambda)M + 28) + \gamma(28\lambda^2 - 33\lambda + 5(2\lambda - 1)M - 5)}{(\gamma - 1)(6\gamma^2 - 20\gamma + 5)M^2}, \\
 a_{2,3}^{\{\mathfrak{f}, \mathfrak{s}, \lambda\}} &= -\frac{4\gamma((\lambda - 1)\lambda + 2\gamma^2(M - 1)M + \gamma(\lambda + (2 - 4\lambda)M + 1))}{(\gamma - 1)(6\gamma^2 - 20\gamma + 5)M^2}, \\
 a_{3,1}^{\{\mathfrak{f}, \mathfrak{s}, \lambda\}} &= \frac{-36\gamma^5 + 252\gamma^4 + 20\lambda^2 - 4\gamma^3(8M^2 + 6\lambda M + 129)}{4(\gamma - 1)(6\gamma^2 - 20\gamma + 5)M^2} \\
 &\quad + \frac{24\gamma^2(\lambda^2 + 5\lambda M + 13) + \gamma(-96\lambda^2 + 60\lambda M - 69) - 20\lambda M + 5}{4(\gamma - 1)(6\gamma^2 - 20\gamma + 5)M^2}, \\
 a_{3,2}^{\{\mathfrak{f}, \mathfrak{s}, \lambda\}} &= \frac{36\gamma^5 - 276\gamma^4 - 5(4\lambda^2 + 1) + \gamma^3(64M^2 + 48\lambda M + 588)}{4(\gamma - 1)(6\gamma^2 - 20\gamma + 5)M^2} \\
 &\quad + \frac{-12\gamma^2(2\lambda^2 + 24\lambda M + 29) + \gamma(112\lambda^2 + 40\lambda M + 73)}{4(\gamma - 1)(6\gamma^2 - 20\gamma + 5)M^2}, \\
 a_{3,3}^{\{\mathfrak{f}, \mathfrak{s}, \lambda\}} &= \frac{\gamma(6\gamma^3 - 4\lambda^2 - 2\gamma^2(4M^2 + 9) + \gamma(16\lambda M + 9) - 1)}{(\gamma - 1)(6\gamma^2 - 20\gamma + 5)M^2}.
 \end{aligned} \tag{37}$$

Despite the stability issues observed at second order, we also consider a third order implicit multirate method with Kværnø–Rentrop coupling using the following algebraically stable base method from [15]:

$$\begin{array}{c|cc}
 \gamma & \gamma \\
 \hline
 1 - \gamma & 1 - 2\gamma & \gamma \\
 \hline
 & 1/2 & 1/2
 \end{array}, \quad \gamma = \frac{3 + \sqrt{3}}{6}. \tag{38}$$

Following the approach in [14,9], the slow to fast coupling is chosen to be

$$A^{\{\mathfrak{f}, \mathfrak{s}, \lambda+1\}} = \frac{1}{M} \left(A^{\{\mathfrak{f}, \mathfrak{s}\}} + F(\lambda) \right),$$

$$F(\lambda) = \mathbb{1}_{s^{\{\mathfrak{f}\}}} [\eta_1(\lambda) \dots \eta_{s^{\{\mathfrak{s}\}}}(\lambda)], \quad \lambda = 0, \dots, M-1,$$

where the η_j satisfy $\sum_{j=1}^{s^{\{\mathfrak{s}\}}} \eta_j(\lambda) = \lambda$. This results in the internal consistency condition reducing to

$$A^{\{\mathfrak{f}, \mathfrak{s}\}} \mathbb{1}_{s^{\{\mathfrak{s}\}}} = c, \quad (40)$$

and the third order coupling condition becoming

$$\frac{M}{6} = b^T \left(A^{\{\mathfrak{f}, \mathfrak{s}\}} + \frac{1}{M} \sum_{\lambda=1}^M F(\lambda) \right) c. \quad (41)$$

At third order, this approach creates coefficients that grow unbounded with M . Moreover, we were unable to find an $A(0^\circ)$ -stable method satisfying the constraints eqs. (40) and (41).

5.4 Fourth order

For the compound-step method of order four, we start with a new base method, solving the coupling and base conditions together. This allows more flexibility to keep the coupling coefficients bounded functions of λ and M . The following L-stable base method was derived:

$\frac{1}{4}$	$\frac{1}{4}$	0	0	0	0
1	$\frac{3}{4}$	$\frac{1}{4}$	0	0	0
$\frac{2}{5}$	$\frac{69}{400}$	$-\frac{9}{400}$	$\frac{1}{4}$	0	0
$\frac{7}{11}$	$\frac{103241}{143748}$	$-\frac{1751}{71874}$	$-\frac{11050}{35937}$	$\frac{1}{4}$	0
1	$\frac{400}{459}$	$-\frac{35}{216}$	$-\frac{250}{351}$	$\frac{1331}{1768}$	$\frac{1}{4}$
	$\frac{400}{459}$	$-\frac{35}{216}$	$-\frac{250}{351}$	$\frac{1331}{1768}$	$\frac{1}{4}$
	$\frac{10388}{10557}$	$-\frac{1399}{4968}$	$-\frac{30425}{32292}$	$\frac{73205}{81328}$	$\frac{125}{368}$

When paired with the following coupling coefficients, we have the compound-step MrGARK SDIRK 4 scheme:

$$\begin{aligned}
a_{1,1}^{\{i,s,\lambda\}} &= \frac{-165(64\lambda^4 - 192\lambda^3 + 240\lambda^2 - 148\lambda + 37) + 2688(4\lambda - 3)M^3 - 3408(8\lambda^2 - 12\lambda + 5)M^2 + 448(64\lambda^3 - 144\lambda^2 + 120\lambda - 37)M}{1836M^4}, \\
a_{1,2}^{\{i,s,\lambda\}} &= \frac{1110(64\lambda^4 - 192\lambda^3 + 240\lambda^2 - 148\lambda + 37) - 1296M^4 - 2292(4\lambda - 3)M^3 + 8781(8\lambda^2 - 12\lambda + 5)M^2 - 2101(64\lambda^3 - 144\lambda^2 + 120\lambda - 37)M}{22464M^4}, \\
a_{1,3}^{\{i,s,\lambda\}} &= -\frac{125(-33(64\lambda^4 - 192\lambda^3 + 240\lambda^2 - 148\lambda + 37) + 336(4\lambda - 3)M^3 - 552(8\lambda^2 - 12\lambda + 5)M^2 + 83(64\lambda^3 - 144\lambda^2 + 120\lambda - 37)M)}{22464M^4}, \\
a_{1,4}^{\{i,s,\lambda\}} &= \frac{1331(-5(64\lambda^4 - 192\lambda^3 + 240\lambda^2 - 148\lambda + 37) + 32(4\lambda - 3)M^3 - 60(8\lambda^2 - 12\lambda + 5)M^2 + 11(64\lambda^3 - 144\lambda^2 + 120\lambda - 37)M)}{56576M^4}, \\
a_{1,5}^{\{i,s,\lambda\}} &= -\frac{85(64\lambda^4 - 192\lambda^3 + 240\lambda^2 - 148\lambda + 37) + 192M^4 + 16(4\lambda - 3)M^3 - 648(8\lambda^2 - 12\lambda + 5)M^2 + 175(64\lambda^3 - 144\lambda^2 + 120\lambda - 37)M}{3328M^4}, \\
a_{2,1}^{\{i,s,\lambda\}} &= -\frac{165(64\lambda^4 - 48\lambda^2 + 68\lambda - 17) + 10752\lambda M^3 - 3408(8\lambda^2 - 1)M^2 + 448(64\lambda^3 - 24\lambda + 17)M}{1836M^4}, \\
a_{2,2}^{\{i,s,\lambda\}} &= \frac{1110(64\lambda^4 - 48\lambda^2 + 68\lambda - 17) - 1296M^4 - 9168\lambda M^3 + 8781(8\lambda^2 - 1)M^2 - 2101(64\lambda^3 - 24\lambda + 17)M}{22464M^4}, \\
a_{2,3}^{\{i,s,\lambda\}} &= -\frac{125(-33(64\lambda^4 - 48\lambda^2 + 68\lambda - 17) + 1344\lambda M^3 - 552(8\lambda^2 - 1)M^2 + 83(64\lambda^3 - 24\lambda + 17)M)}{22464M^4}, \\
a_{2,4}^{\{i,s,\lambda\}} &= \frac{1331(5(-64\lambda^4 + 48\lambda^2 - 68\lambda + 17) + 128\lambda M^3 - 60(8\lambda^2 - 1)M^2 + 11(64\lambda^3 - 24\lambda + 17)M)}{56576M^4}, \\
a_{2,5}^{\{i,s,\lambda\}} &= -\frac{85(64\lambda^4 - 48\lambda^2 + 68\lambda - 17) + 192M^4 + 64\lambda M^3 - 648(8\lambda^2 - 1)M^2 + 175(64\lambda^3 - 24\lambda + 17)M}{3328M^4}, \\
a_{3,1}^{\{i,s,\lambda\}} &= -\frac{33(32000\lambda^4 - 76800\lambda^3 + 84720\lambda^2 - 56180\lambda + 15773) + 215040(5\lambda - 3)M^3}{183600M^4} \\
&\quad + \frac{-3408(800\lambda^2 - 960\lambda + 353)M^2 + 448(6400\lambda^3 - 11520\lambda^2 + 8472\lambda - 2809)M}{183600M^4}, \\
a_{3,2}^{\{i,s,\lambda\}} &= \frac{222(32000\lambda^4 - 76800\lambda^3 + 84720\lambda^2 - 56180\lambda + 15773) - 129600M^4 - 183360(5\lambda - 3)M^3}{2246400M^4} \\
&\quad + \frac{8781(800\lambda^2 - 960\lambda + 353)M^2 - 2101(6400\lambda^3 - 11520\lambda^2 + 8472\lambda - 2809)M}{2246400M^4}, \\
a_{3,3}^{\{i,s,\lambda\}} &= \frac{33(32000\lambda^4 - 76800\lambda^3 + 84720\lambda^2 - 56180\lambda + 15773) - 134400(5\lambda - 3)M^3}{89856M^4} \\
&\quad + \frac{2760(800\lambda^2 - 960\lambda + 353)M^2 - 415(6400\lambda^3 - 11520\lambda^2 + 8472\lambda - 2809)M}{89856M^4}, \\
a_{3,4}^{\{i,s,\lambda\}} &= \frac{1331(-32000\lambda^4 + 76800\lambda^3 - 84720\lambda^2 + 56180\lambda + 2560(5\lambda - 3)M^3)}{5657600M^4} \\
&\quad + \frac{1331(-60(800\lambda^2 - 960\lambda + 353)M^2 + 11(6400\lambda^3 - 11520\lambda^2 + 8472\lambda - 2809)M - 15773)}{5657600M^4}, \\
a_{3,5}^{\{i,s,\lambda\}} &= -\frac{17(32000\lambda^4 - 76800\lambda^3 + 84720\lambda^2 - 56180\lambda + 15773) + 19200M^4 + 1280(5\lambda - 3)M^3}{332800M^4} \\
&\quad + \frac{-648(800\lambda^2 - 960\lambda + 353)M^2 + 175(6400\lambda^3 - 11520\lambda^2 + 8472\lambda - 2809)M}{332800M^4}, \\
a_{4,1}^{\{i,s,\lambda\}} &= -\frac{33(425920\lambda^4 - 619520\lambda^3 + 280720\lambda^2 - 35660\lambda + 2387) + 1300992(11\lambda - 4)M^3}{2443716M^4} \\
&\quad + \frac{-137456(264\lambda^2 - 192\lambda + 29)M^2 + 448(85184\lambda^3 - 92928\lambda^2 + 28072\lambda - 1783)M}{2443716M^4}, \\
a_{4,2}^{\{i,s,\lambda\}} &= \frac{222(425920\lambda^4 - 619520\lambda^3 + 280720\lambda^2 - 35660\lambda + 2387) - 1724976M^4 - 1109328(11\lambda - 4)M^3}{29899584M^4} \\
&\quad + \frac{354167(264\lambda^2 - 192\lambda + 29)M^2 - 2101(85184\lambda^3 - 92928\lambda^2 + 28072\lambda - 1783)M}{29899584M^4}, \\
a_{4,3}^{\{i,s,\lambda\}} &= -\frac{25(-33(425920\lambda^4 - 619520\lambda^3 + 280720\lambda^2 - 35660\lambda + 2387) + 813120(11\lambda - 4)M^3)}{29899584M^4} \\
&\quad - \frac{25(-111320(264\lambda^2 - 192\lambda + 29)M^2 + 415(85184\lambda^3 - 92928\lambda^2 + 28072\lambda - 1783)M)}{29899584M^4}, \\
a_{4,4}^{\{i,s,\lambda\}} &= -\frac{425920\lambda^4 + 619520\lambda^3 - 280720\lambda^2 - 35660\lambda + 15488(11\lambda - 4)M^3}{56576M^4} \\
&\quad + \frac{-2420(264\lambda^2 - 192\lambda + 29)M^2 + 11(85184\lambda^3 - 92928\lambda^2 + 28072\lambda - 1783)M - 2387}{56576M^4}, \\
a_{4,5}^{\{i,s,\lambda\}} &= -\frac{17(425920\lambda^4 - 619520\lambda^3 + 280720\lambda^2 - 35660\lambda + 2387) + 255552M^4 + 7744(11\lambda - 4)M^3}{4429568M^4} \\
&\quad + \frac{-26136(264\lambda^2 - 192\lambda + 29)M^2 + 175(85184\lambda^3 - 92928\lambda^2 + 28072\lambda - 1783)M}{4429568M^4}, \\
a_{5,1}^{\{i,s,\lambda\}} &= \frac{16\lambda(-165\lambda^3 + 168\lambda^2 - 426\lambda M^2 + 448\lambda^2 M)}{459M^4}, \\
a_{5,2}^{\{i,s,\lambda\}} &= -\frac{-8880\lambda^4 + 162M^4 + 1146\lambda M^3 - 8781\lambda^2 M^2 + 16808\lambda^3 M}{2808M^4}, \\
a_{5,3}^{\{i,s,\lambda\}} &= \frac{125\lambda(33\lambda^3 - 21M^3 + 69\lambda M^2 - 83\lambda^2 M)}{351M^4}, \\
a_{5,4}^{\{i,s,\lambda\}} &= \frac{1331\lambda(-10\lambda^3 + 4M^3 - 15\lambda M^2 + 22\lambda^2 M)}{1768M^4}, \\
a_{5,5}^{\{i,s,\lambda\}} &= \frac{-85\lambda^4 + 3M^4 + \lambda M^3 - 81\lambda^2 M^2 + 175\lambda^3 M}{52M^4}.
\end{aligned} \tag{42}$$

The scalar stability of compound-step methods eqs. (36), (37) and (42) are summarized in table 1. In all cases, the methods are just a few degrees short of scalar L-stability. As M increases, the stability angles decrease by less than 2° before stabilizing.

Method	$M = 2$	$M = 3$	$M = 4$	$M = 8$	$M = 16$	$M = 32$
SDIRK 2 (from eq. (36))	84.6°	83.5°	83.2°	83.0°	83.0°	83.0°
SDIRK 3 (from eq. (37))	88.6°	87.8°	87.3°	86.9°	86.8°	86.8°
SDIRK 4 (from eq. (42))	81.7°	81.2°	81.2°	81.2°	81.2°	81.2°

Table 1 Scalar $L(\alpha)$ -stability (as defined in definition 2) for new compound-step MrGARK methods.

6 Numerical Experiments

In this section, we use the new methods to integrate two test problems. First, the Gray–Scott model is used to verify the order of accuracy. Then, the inverter chain model, is used to compare the performance of multirate methods against single rate ones.

6.1 Gray–Scott model

The Gray–Scott equation describes the reaction and diffusion of two chemical species [16]:

$$\underbrace{\begin{bmatrix} U \\ V \end{bmatrix}}_{y'}' = \underbrace{\begin{bmatrix} D_u \nabla^2 U \\ D_v \nabla^2 V \end{bmatrix}}_{f^{\{s\}}(y)} + \underbrace{\begin{bmatrix} -U V^2 + F(1 - U) \\ U V^2 - (F + k)V \end{bmatrix}}_{f^{\{f\}}(y)}. \quad (43)$$

The spacial domain is periodic over $[0, 2.5] \times [0, 2.5]$, the timespan is $[0, 500]$, and the parameters are $D_u = 2 \times 10^{-5}$, $D_v = 10^{-5}$, $F = 0.034$, and $k = 0.054$. Second order central differences are used to discretize the domain into a 64×64 grid. The diffusion terms form the slow partition, and the reaction terms form the fast partition. Errors are computed against a reference solution at the final integration time. We note this problem is challenging for multirate methods in the sense that the partitions are tightly coupled. Convergence plots are provided in fig. 2. In all cases, the theoretical orders are achieved for multirate ratios $M = 2, 4, 6$.

6.2 Inverter chain model

We also consider the inverter chain model of [14] given by the equations

$$\begin{aligned} U'_1 &= U_{op} - U_1 - g(U_{in}, U_1, U_0), \\ U'_i &= U_{op} - U_i - g(U_{i-1}, U_i, U_0), \quad i = 2, \dots, m, \end{aligned} \quad (44)$$

with

$$g(U_g, U_D, U_S) = (\max(U_g - U_S - U_T, 0))^2 - (\max(U_g - U_D - U_T, 0))^2.$$

The ground voltage is $U_0 = 0$, the operating voltage is $U_{op} = 5$, and the threshold voltage separating the on and off states is $U_T = 1$. The initial conditions of the system are

$$U_i(0) = \begin{cases} 6.246 \times 10^{-3} & j \text{ even} \\ 5 & j \text{ odd} \end{cases},$$

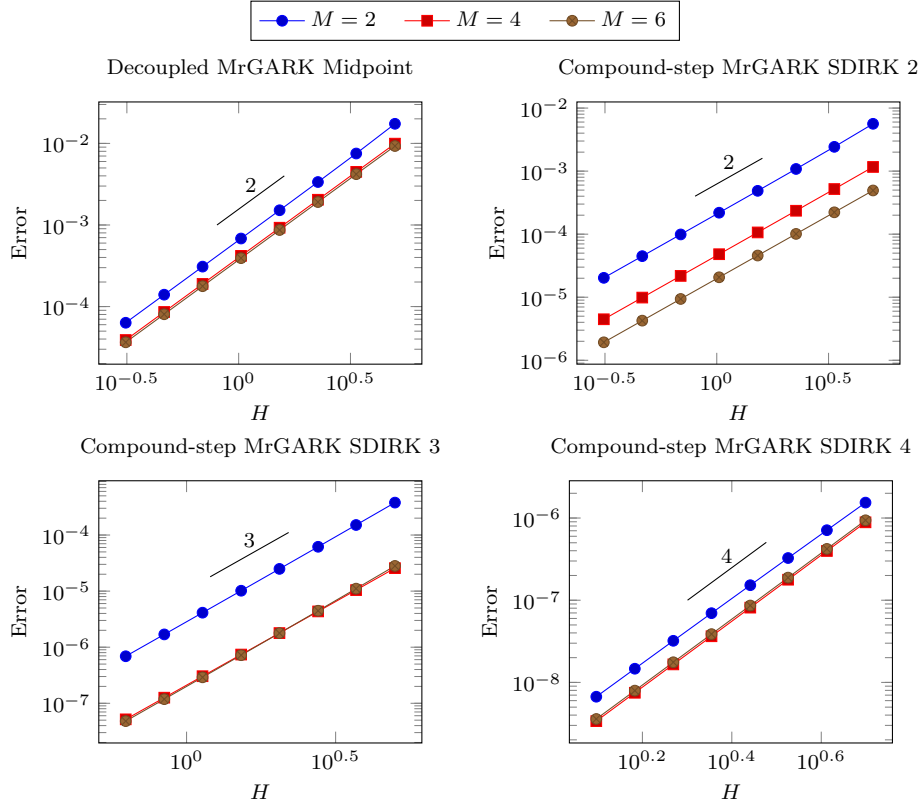


Fig. 2 Error vs. macro-step H for the decoupled midpoint method eq. (35) and compound-step methods eqs. (36), (37) and (42) applied to the Gray–Scott problem eq. (43). Reference slopes are included to confirm the theoretical orders.

and the input signal is taken to be

$$U_{in}(t) = \begin{cases} t - 5 & 5 \leq t \leq 10 \\ 5 & 10 \leq t \leq 15 \\ \frac{5}{2}(17 - t) & 15 \leq t \leq 17 \\ 0 & \text{otherwise} \end{cases}.$$

For the numerical experiments, we use $m = 200$ and a timespan of $[0, 140]$ to allow the signal to reach the end of the chain.

We use the inverter chain problem to compare the new compound-step multirate methods to their single rate base methods. As the signal propagates through the chain, the fast components change and are adaptively selected using the technique described in section 2.2. Across the entire timespan, the number of fast variables is a small fraction of the total number of variables. The speedup one can expect depends heavily on the implementation details including the programming language, choice of linear solver, Newton's method tolerances, and stage value predictors. We expect the overall cost of the integration to be dominated by the Newton iterations since each iterate requires a function evaluation and a linear

solve. For this problem, the Jacobian is bidiagonal and the linear solve cost scales linearly with the dimension. As an idealized measure of work, similar to that in [25], we accumulate the dimension of every linear solve performed across the entire integration. This work quantity is equivalent to the number of component function evaluations.

In order to measure the multirate performance and efficiency, we sweep through a range of step sizes and determine the amount of work and error for each run. This is plotted in fig. 3 for several multirate ratios. In all cases, the multirate methods are more efficient than the single rate base methods, often decreasing error by orders of magnitude for a fixed amount of work. The improvement, however, depends on the choice of multirate ratio. Small values call the slow partition too infrequently and limit efficiency. On the other hand, as multirate ratio increases, at some point the fast partition is resolved accurately enough that fast errors become negligible compared to the slow and coupling errors, and further increasing M only increases the work. Note also that as the order of the method increases, the optimal multirate ratio decreases.

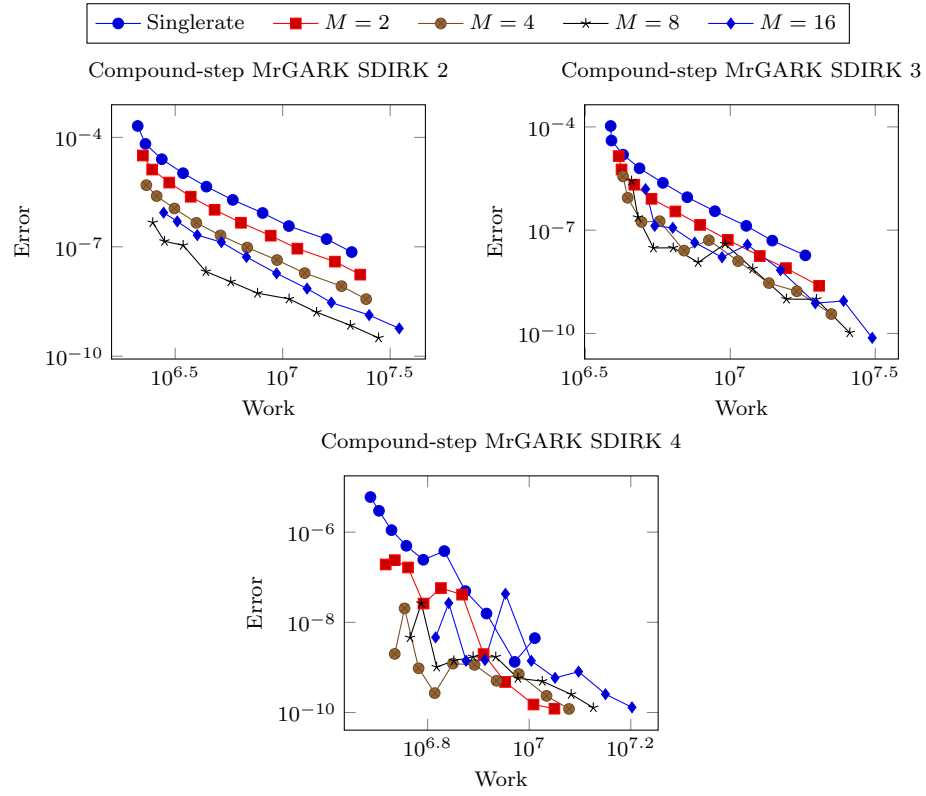


Fig. 3 Error vs. work for the compound-step methods eqs. (36), (37) and (42) applied to the inverter chain problem eq. (44)

We note the results in fig. 3 assume the cost of linear solves dominates any overhead associated with the implementation of the multirate methods. Realizing this in an implementation would require efficient means to evaluate the right-hand side and Jacobian on a subset of variables, as well as optimizations such as precomputing $A^{\{j,s,\lambda\}}$ for appropriate values of λ and M . Problems where the cost of linear solves scales quadratically or cubically with the dimension would likely see the greatest advantage from multirate methods.

7 Conclusions

In this work, we have explored multirate Runge–Kutta methods in which all timescales are treated implicitly. By taking different timesteps for different partitions of an ODE, these methods can more efficiently integrate stiff, multiscale problems.

Compared to single rate methods, the linear stability for multirate methods is much more intricate. It not only depends on the base methods and coupling structure, but also the choice of test problem. The scalar and 2D test problems present a tradeoff of generality versus simplicity to analyze. Much of the theoretical limitations and observed degradation of multirate stability comes from problems that are oscillatory. These problems are challenging because the error introduced by the coupling is not damped by any partition. In addition, we found that forgoing internal consistency can improve stability, but increases the number of order conditions and limits the stage order to zero.

The coupling structure of MrGARK methods has a significant effect on the computational cost of the Newton iterations. Decoupled methods are the cheapest and simplest to implement, especially for component partitioned problems. Coupled methods have the potential to become prohibitively expensive but can be implemented efficiently by exploiting stage reducibility or low rank structure in the method.

The GARK framework provides new insight into the compound-step methods. Instead of taking the approach of finding a dense output formula for coupling, we use the precise GARK order conditions. This approach facilitated the development of methods up to order four, which to our knowledge, is the highest of this type. Stability depends heavily on this coupling, so we derived a practical and general form for the scalar stability function. By taking the limit as the partitions become infinitely stiff, we found a simple condition to ensure $L(\alpha)$ -stability.

New standard MrGARK methods based on backward Euler and the midpoint method show excellent stability properties. For base methods with more than one stage, however, we were unable to find methods with satisfactory stability. Extrapolation may be the most practical way to achieve high-order, but this warrants additional investigation.

Numerical experiments with Gray–Scott model validate the correctness of the order conditions and the methods. Finally, performance results with the inverter chain problem show orders of magnitude improvements in error for fixed work when compared to the single rate base methods.

Acknowledgements

The work of S. Roberts (in part), J. Loffeld, and C.S Woodward was supported by the Lawrence Livermore Laboratory Directed Research and Development Program under tracking number 17-ERD-035. Their work was performed under the auspices of the U.S. Department of Energy by Lawrence Livermore National Laboratory under contract DE-AC52-07NA27344. Lawrence Livermore National Security, LLC. LLNL-JRNL-795454. The work of S. Roberts (in part), A. Sarshar, and A. Sandu is supported by awards NSF CCF-1613905, NSF ACI-1709727, AFOSR DDDAS FA9550-17-1-0015, and by the Computational Science Laboratory at Virginia Tech.

The authors thank Jeffrey Hittinger and Valentin Dallerit for helpful discussions.

This document was prepared as an account of work sponsored by an agency of the United States government. Neither the United States government nor Lawrence Livermore National Security, LLC, nor any of their employees makes any warranty, expressed or implied, or assumes any legal liability or responsibility for the accuracy, completeness, or usefulness of any information, apparatus, product, or process disclosed, or represents that its use would not infringe privately owned rights. Reference herein to any specific commercial product, process, or service by trade name, trademark, manufacturer, or otherwise does not necessarily constitute or imply its endorsement, recommendation, or favoring by the United States government or Lawrence Livermore National Security, LLC. The views and opinions of authors expressed herein do not necessarily state or reflect those of the United States government or Lawrence Livermore National Security, LLC, and shall not be used for advertising or product endorsement purposes.

References

1. Alexander, R.: Diagonally implicit Runge–Kutta methods for stiff ODEs. *SIAM Journal on Numerical Analysis* **14**(6), 1006–1021 (1977). DOI 10.1137/0714068
2. Andrus, J.: Stability of a multi-rate method for numerical integration of ODEs. *Computers & Mathematics with applications* **25**(2), 3–14 (1993)
3. Bonaventura, L., Casella, F., Delpopolo, L., Ranade, A.: A self adjusting multirate algorithm based on the TR-BDF2 method. *arXiv preprint arXiv:1801.09118* (2018)
4. Constantinescu, E.M., Sandu, A.: Extrapolated multirate methods for differential equations with multiple time scales. *Journal of Scientific Computing* **56**(1), 28–44 (2013). DOI 10.1007/s10915-012-9662-z
5. Delpopolo Carciopolo, L., Bonaventura, L., Scotti, A., Formaggia, L.: A conservative implicit multirate method for hyperbolic problems. *Computational Geosciences* (2018). DOI 10.1007/s10596-018-9764-2
6. Gear, C.: Multirate methods for ordinary differential equations. Tech. rep., Illinois Univ., Urbana (USA). Dept. of Computer Science (1974)
7. Gear, C.W., Wells, D.: Multirate linear multistep methods. *BIT Numerical Mathematics* **24**(4), 484–502 (1984)
8. Günther, M., Rentrop, P.: Multirate ROW methods and latency of electric circuits. *Applied Numerical Mathematics* **13**(1), 83 – 102 (1993). DOI [https://doi.org/10.1016/0168-9274\(93\)90133-C](https://doi.org/10.1016/0168-9274(93)90133-C)
9. Günther, M., Sandu, A.: Multirate generalized additive Runge–Kutta methods. *Numerische Mathematik* **133**(3), 497–524 (2016). DOI 10.1007/s00211-015-0756-z
10. Hachtel, C., Bartel, A., Gnther, M., Sandu, A.: Multirate implicit Euler schemes for a class of differential-algebraic equations of index-1. *Journal of Computational and Applied Mathematics* p. 112499 (2019). DOI 10.1016/j.cam.2019.112499

11. Hairer, E., Wanner, G.: Solving ordinary differential equations II: Stiff and differential-algebraic problems, 2 edn. No. 14 in Springer Series in Computational Mathematics. Springer-Verlag Berlin Heidelberg (1996)
12. Hundsdorfer, W., Savcenco, V.: Analysis of a multirate Theta-method for stiff ODEs. *Appl. Numer. Math.* **59**(3-4), 693–706 (2009). DOI 10.1016/j.apnum.2008.03.022
13. Kværnø, A.: Stability of multirate Runge–Kutta schemes (2000). DOI 10.1.1.40.8965
14. Kværnø, A., Rentrop, P.: Low order multirate Runge–Kutta methods in electric circuit simulation (1999). DOI 10.1.1.9.3084
15. Norsett, S.P.: Semi explicit Runge–Kutta methods. Matematisk Institut, Universitet I (1974)
16. Pearson, J.E.: Complex patterns in a simple system. *Science* **261**(5118), 189–192 (1993). DOI 10.1126/science.261.5118.189
17. Rice, J.R.: Split Runge–Kutta methods for simultaneous equations. *Journal of Research of the National Institute of Standards and Technology* **60** (1960)
18. Roberts, S., Sarshar, A., Sandu, A.: Coupled multirate infinitesimal GARK schemes for stiff systems with multiple time scales. arXiv preprint arXiv:1812.00808 (2018)
19. Rodríguez-Gómez, G., González-Casanova, P., Martínez-Carballido, J.: Computing general companion matrices and stability regions of multirate methods. *International journal for numerical methods in engineering* **61**(2), 255–273 (2004)
20. Sand, J., Skelboe, S.: Stability of backward Euler multirate methods and convergence of waveform relaxation. *BIT Numerical Mathematics* **32**(2), 350–366 (1992)
21. Sandu, A.: A class of multirate infinitesimal gark methods. *SIAM Journal on Numerical Analysis* **57**(5), 2300–2327 (2019). DOI 10.1137/18M1205492
22. Sandu, A., Günther, M.: A generalized-structure approach to additive Runge–Kutta methods. *SIAM Journal on Numerical Analysis* **53**(1), 17–42 (2015). DOI 10.1137/130943224
23. Sarshar, A., Roberts, S., Sandu, A.: Design of high-order decoupled multirate GARK schemes. *SIAM Journal on Scientific Computing* **41**(2), A816–A847 (2019). DOI 10.1137/18M1182875
24. Savcenco, V.: Comparison of the asymptotic stability properties for two multirate strategies. *Journal of Computational and Applied Mathematics* **220**(1-2), 508–524 (2008)
25. Savcenco, V., Hundsdorfer, W., Verwer, J.: A multirate time stepping strategy for stiff ordinary differential equations. *BIT Numerical Mathematics* **47**(1), 137–155 (2007)
26. Scheidemann, V.: Introduction to complex analysis in several variables. Springer (2005)
27. Sexton, J.M., Reynolds, D.R.: Relaxed multirate infinitesimal step methods. arXiv preprint arXiv:1808.03718 (2018). Submitted to *J. Comput. Appl. Math.*
28. Skelboe, S., Andersen, P.U.: Stability properties of backward Euler multirate formulas. *SIAM journal on scientific and statistical computing* **10**(5), 1000–1009 (1989)
29. Strang, G.: On the construction and comparison of difference schemes. *SIAM journal on numerical analysis* **5**(3), 506–517 (1968)
30. Verhoeven, A., Beelen, T., El Guennouni, A., ter Maten, E., Mattheij, R., Tasić, B., et al.: Error analysis of BDF compound-fast multirate method for differential-algebraic equations (2006)
31. Verhoeven, A., El Guennouni, A., Ter Maten, E., Mattheij, R.: A general compound multirate method for circuit simulation problems. In: *Scientific Computing in Electrical Engineering*, pp. 143–149. Springer (2006)
32. Verhoeven, A., Ter Maten, E.J.W., Mattheij, R.M., Tasić, B.: Stability analysis of the BDF slowest-first multirate methods. *International Journal of Computer Mathematics* **84**(6), 895–923 (2007)
33. Zhao, D., Li, Y., Barbić, J.: Asynchronous implicit backward Euler integration. In: *Proceedings of the ACM SIGGRAPH/Eurographics Symposium on Computer Animation, SCA '16*, pp. 1–9. Eurographics Association, Goslar Germany, Germany (2016). URL <http://dl.acm.org/citation.cfm?id=2982818.2982820>